ESC European Society of Cardiology

European Heart Journal - Cardiovascular Imaging (2017) **18**, 1090–1091
doi:10.1093/ehjci/jex034

POSITION PAPER

Multimodality Imaging in Restrictive Cardiomyopathies: An EACVI expert consensus document In collaboration with the "Working Group on myocardial and pericardial diseases" of the European Society of Cardiology Endorsed by The Indian Academy of Echocardiography

Gilbert Habib[1,2]*, Chiara Bucciarelli-Ducci[3], Alida L.P. Caforio[4], Nuno Cardim[5], Philippe Charron[6,7], Bernard Cosyns[8], Aurélie Dehaene[9], Genevieve Derumeaux[10], Erwan Donal[11], Marc R. Dweck[12], Thor Edvardsen[13,14], Paola Anna Erba[15], Laura Ernande[10], Oliver Gaemperli[16], Maurizio Galderisi[17], Julia Grapsa[18], Alexis Jacquier[19], Karin Klingel[20], Patrizio Lancellotti[21,22], Danilo Neglia[23], Alessia Pepe[24], Pasquale Perrone-Filardi[17], Steffen E. Petersen[25], Sven Plein[26], Bogdan A. Popescu[27], Patricia Reant[28], L. Elif Sade[29], Erwan Salaun[30], Riemer H.J.A. Slart[31,32], Christophe Tribouilloy[33], and Jose Zamorano[34]

Reviewers: Victoria Delgado, Kristina Haugaa (EACVI Scientific Documents Committee) and G Vijayaraghavan (Indian Academy of Echocardiography)

[1]Aix- Aix-Marseille Univ, URMITE, Aix Marseille Université—UM63, CNRS 7278, IRD 198, INSERM 1095; [2]Cardiology Department, APHM, La Timone Hospital, Boulevard Jean Moulin, 13005 Marseille, France; [3]Bristol Heart Institute, National Institute of Health Research (NIHR) Bristol Cardiovascular Biomedical Research Unit (BRU), University of Bristol, Bristol, UK; [4]Cardiology, Department of Cardiological Thoracic and Vascular Sciences, University of Padova, Italy; [5]Multimodality Cardiac Imaging Department, Sports Cardiology and Cardiomyopathies Centre-Hospital da Luz; Lisbon, Portugal; [6]Université Versailles Saint Quentin, INSERM U1018, Hôpital Ambroise Paré, Boulogne-Billancourt, France; [7]Centre de référence pour les maladies cardiaques héréditaires, APHP, ICAN, Hôpital de la Pitié Salpêtrière, Paris, France; [8]CHVZ (Centrum voor Hart en Vaatziekten—UZ Brussel; [9]Department of Radiology and Cardiovascular Imaging, APHM, Hôpitaux de la Timone, Pôle d'imagerie Médicale, 13005 Marseille, France; [10]Department of Physiology, INSERM U955, Université Paris-Est Creteil, Henri Mondor Hospital, DHU-ATVB, AP-HP, Créteil, France; [11]Cardiologie—CHU Rennes & CIC-IT 1414 & LTSI INSERM 1099 – Université Rennes-1; [12]Centre for Cardiovascular Science, University of Edinburgh; [13]Department of Cardiology, Center for Cardiological Innovation and Institute for Surgical Research, Oslo University Hospital, Oslo, Norway; [14]University of Oslo, Oslo, Norway; [15]Regional Center of Nuclear Medicine, Department of Translational Research and New Technology in Medicine, University of Pisa, Pisa, Italy; [16]University Heart Center Zurich, Interventional Cardiology and Cardiac Imaging 19, Zurich; [17]Department of Advanced Biomedical Sciences, Federico II University, Naples, Italy; [18]Department of Cardiovascular Sciences, Imperial College of London, London, UK; [19]Department of Radiology and Cardiovascular Imaging, APHM, Hôpitaux de la Timone, Pôle d'imagerie Médicale, Aix-Marseille Université, CNRS, CRMBM UMR 7339, 13385 Marseille, France; [20]Department of Molecular Pathology, Institute for Pathology and Neuropathology, University Hospital Tuebingen, Tuebingen, Germany; [21]Departments of Cardiology, Heart Valve Clinic, University of Liège Hospital, GIGA Cardiovascular Sciences, CHU Sart Tilman, Liège, Belgium; [22]Gruppo Villa Maria Care and Research, Anthea Hospital, Bari, Italy; [23]Cardiovascular Department, Fondazione Toscana G. Monasterio, CNR Institute of Clinical Physiology, Scuola Superiore Sant'Anna, Pisa, Italy; [24]Magnetic Resonance Imaging Unit, Fondazione G. Monasterio C.N.R.—Regione Toscana Pisa, Italy; [25]Department of Advanced Cardiovascular Imaging, William Harvey Research Institute, National Institute for Health Research Cardiovascular Biomedical Research Unit at Barts, London, UK; [26]Division of Biomedical Imaging, Multidisciplinary Cardiovascular Research Centre, Leeds Institute of Cardiovascular and Metabolic Medicine LIGHT Laboratories, University of Leeds, UK; [27]University of Medicine and Pharmacy 'Carol Davila'—Euroecolab, Institute of Cardiovascular Diseases, Bucharest, Romania; [28]CHU de Bordeaux, Bordeaux, France; [29]Baskent University, Ankara, Turkey; [30]Cardiology Department, La Timone Hospital, Marseille France; [31]Department of Nuclear Medicine and Molecular Imaging, University of Groningen, University Medical Center Groningen, Hanzeplein 1, Groningen, The Netherlands; [32]Department of Biomedical Photonic Imaging, University of Twente, PO Box 217, 7500 AEEnschede, The Netherlands; [33]Department of

*Corresponding author. Tel: 00 33 (0)4 91 38 75 88; Fax: 00 33 (0)4 91 38 47 64. Email: gilbert.habib3@gmail.com

Cardiology, University Hospital Amiens, Amiens, France and INSERM U-1088, Jules Verne University of Picardie, Amiens, France; and [34]University Hospital Ramon y Cajal Carretera de Colmenar Km 9,100, 28034 Madrid, Spain

Received 9 February 2017; editorial decision 13 February 2017; accepted 14 February 2017; online publish-ahead-of-print 16 May 2017

Restrictive cardiomyopathies (RCMs) are a diverse group of myocardial diseases with a wide range of aetiologies, including familial, genetic and acquired diseases and ranging from very rare to relatively frequent cardiac disorders. In all these diseases, imaging techniques play a central role. Advanced imaging techniques provide important novel data on the diagnostic and prognostic assessment of RCMs. This EACVI consensus document provides comprehensive information for the appropriateness of all non-invasive imaging techniques for the diagnosis, prognostic evaluation, and management of patients with RCM.

Keywords echocardiography • cardiac magnetic resonance • computed tomography • nuclear imaging • cardiomyopathies • restrictive cardiomyopathies

Table of Contents

Introduction

Restrictive cardiomyopathies (RCMs) are a diverse group of myocardial diseases with a wide range of aetiologies including familial, genetic, and acquired diseases and ranging from very rare to relatively frequent cardiac disorders. This diversity is also reflected in the inconsistent classification of RCM across guidelines[1–3] and even in the term 'restrictive', which is a functional characterization, unlike the morphological definition of the three other main types of cardiomyopathies, i.e. hypertrophic, arrhythmogenic right ventricular or dilated cardiomyopathies.[4]

Independently of the underlying cause, the pathophysiology, and clinical presentation, the initial phenotypic diagnosis of RCM requires imaging techniques. Many advances have occurred in the last decade in the diagnostic and prognostic assessment of RCM. This EACVI consensus document provides comprehensive information for the appropriateness of all non-invasive imaging techniques for the diagnosis, prognostic evaluation, and management of patients with RCM.

This article was written in close collaboration between the European Association of Cardiovascular Imaging (EACVI) and the Working Group (WG) on Myocardial and Pericardial diseases of the European Society of Cardiology (ESC). The types of RCM covered in this document are those included in the classification system proposed by the WG on Myocardial and Pericardial diseases[1] as well as some non-sarcomeric hypertrophic cardiomyopathies (HCMs) with a restrictive physiology that in previous classifications were included in the RCM category, e.g. cardiac amyloidosis (CA).

Definition and classification of RCM

RCM is the least common type of the cardiomyopathies, defined as *myocardial disorders in which the heart muscle is structurally and functionally abnormal in the absence of coronary artery disease, arterial systemic hypertension, valvular disease, or congenital heart disease sufficient to cause the observed myocardial abnormality.*[1]

According to the historical World Health Organization (WHO)[2] and the updated definition proposed by the ESC WG on Myocardial and Pericardial Diseases in 2008,[1] each cardiomyopathy type is described by its clinical presentation. This approach is recommended firstly because it is the starting point in everyday clinical practice, and secondly because knowledge of aetiologies is still evolving, thus at present an aetiological classification would not be conclusive.

RCM is defined by restrictive ventricular physiology in the presence of normal or reduced diastolic volumes, with normal or

near-normal left ventricular (LV) systolic function, and normal or near-normal wall thickness.[1–5] Increased interstitial fibrosis may be present. RCM constitutes a heterogeneous group of heart muscle diseases with various causes (*Table 1*) that may be classified according to very different criteria.

According to the main pathophysiological mechanism, RCM may be subclassified into infiltrative or storage diseases (e.g. amyloidosis and glycogen storage disease); obliterative or endomyocardial diseases [e.g. endomyocardial fibrosis (EMF), related or not to hypereosinophilia].

The WHO classification system was based on the distinction between primary and secondary myocardial disorders.[2] Primary cardiomyopathies were defined as either not caused by an identifiable agent, e.g. idiopathic, or related to a primary myocardial cause. Secondary diseases were related to systemic disorders affecting the myocardium with a pathophysiological process starting outside of, e.g. unspecific to the myocardium. The American Heart Association (AHA) proposed a slightly different classification system in which the term 'primary' was used to describe diseases in which the heart is the sole or predominantly involved organ whereas 'secondary' is used to describe diseases in which myocardial dysfunction is part of a systemic disorder.[3]

However, the challenge of distinguishing primary and secondary disorders is illustrated by the fact that many diseases classified as primary cardiomyopathies (e.g. glycogen storage disease, mitochondrial cytopathies) in the AHA classification can be associated with major extra-cardiac manifestations. Conversely, pathology in many of the diseases classified as secondary cardiomyopathies can predominantly (or exclusively) involve the heart (e.g. EMF or Fabry disease cardiac variant). In addition, the term of primary cardiomyopathy as an idiopathic condition is no longer appropriate in a large group of patients since genetics has identified mutations in various genes such as sarcomeric causes. Therefore, the ESC WG on Myocardial & Pericardial Diseases proposed in 2008 to abandon the distinction between primary and secondary causes.[1]

As an alternative to this classification, the ESC Working Group on Myocardial and Pericardial Diseases proposed to subclassify RCM and other cardiomyopathies into (i) familial or genetic causes and (ii) non-familial/non-genetic causes, because of the recent and increasing knowledge about genetic causes of cardiomyopathies. This is especially illustrated in RCM related to CA that may be acquired (amyloidosis AL or senile amyloidosis) or genetically determined (transthyretin and other genes mutations) and be included in the non-sarcomeric HCMs as well as in the RCM.[1] The latter ESC classification will be used in this position paper.

Table 1 Main causes of RCM

Cause	Familial/ genetic	Non-familial/ non-genetic
Apparently Idiopathic		
Genetic origin	X	
Unknown origin		X
Amyloidosis		
AL/prealbumin		X
Genetic (e.g. TTR)	X	
Senile		X
Other infiltrative diseases (such as Gaucher's disease, Hurler's disease)	X	
Inflammatory cardiomyopathies with a restrictive haemodynamic component: Sarcoidosis, SSc		X
Storage diseases		
Haemochromatosis	X	
Fabry disease	X	
Glycogen storage disease	X	
Pseudoxanthoma elasticum	X	
Radiation therapy		X
Drugs		X
Endomyocardial diseases (with or without hypereosinophilia, carcinoid disease, drug induced)	X (rare)	X (frequent)
Miscellaneous (radiation, drug-induced, e.g. antracycline toxicity, serotonin, methysergide, ergotamine, mercurial agents, and busulfan)		X

RCM, restrictive cardiomyopathy; TTR, transthyretin; SSc, systemic sclerosis.

Pathophysiology of RCM and clinical presentation

Restrictive physiology is characterized by a pattern of LV filling in which increased stiffness of the myocardium causes a precipitously rise of LV pressure with only small increases in volume. On cardiac catheterization, this phenomenon is characterized by a dip-and-plateau contour of early diastolic pressure traces. The standard echocardiographic features of 'restrictive' filling are described in Section Echocardiography

Similarly, some patients with a restrictive physiology may have significantly increased wall thickness such as patients with CA. RCM should be differentiated from constrictive pericarditis (CP).[6,7] (see Section Main forms of RCM and value of imaging techniques).

Imaging modalities in RCM

Echocardiography

Echocardiography plays a key role for the recognition of RCM. The echocardiographic diagnosis requires to differentiate RCM from CP.

RCM are usually characterized by normal or small LV cavity size (<40 mL/m^2) with preserved LV ejection fraction, bi-atrial enlargement, and diastolic dysfunction.[5]

Assessment of LV diastolic function and filling pressures is of utmost value in RCM. In the recent joint American Society of Echocardiography (ASE)/EACVI recommendations for the evaluation of diastolic function by echocardiography,[8] the four recommended variables to diagnose LV diastolic dysfunction and their abnormal cut-off values are annular e' velocity (septal e' < 7 cm/s, lateral e' < 10 cm/s), average E/e' ratio > 14, LA maximum volume index > 34 mL/m^2, and peak TR velocity > 2.8 m/s (*Figure 1*). Other valuable parameters to identify the presence of elevated LV filling pressures are the ratio of pulmonary vein peak systolic to peak diastolic velocity, or systolic time

velocity integral to diastolic time velocity integral < 1, and the changes in E/A ratio with Valsalva manoeuver. The restrictive filling is considered reversible if the change of E/A ratio during Valsalva is ≥ 0.5 and fixed if it is < 0.5 (more severe form).

The diagnosis of RCM does not equal the presence of restrictive physiology. Patients with true RCM may present with a Grade I diastolic dysfunction and move progressively to Grade II or III diastolic dysfunction with worsening of their disease. The advanced stages of RCM are characterized by typical restrictive physiology with a mitral inflow E/A ratio > 2.5, DT of E velocity < 150 ms, IVRT < 50 ms, decreased septal and lateral e' velocities (3–4 cm/s), E/e' ratio > 14, as well as a markedly increased LA volume index (>50 mL/m^2),[8] this advanced restrictive pattern being associated with the worst prognosis.[9] Wall thickness is usually normal.

Some specific features may also help differentiate secondary RCM, including several systemic conditions (diabetic cardiomyopathy, scleroderma, EMF, radiation, chemotherapy, carcinoid heart disease, metastatic cancers), from apparently idiopathic RCM (see Section Main forms of RCM and value of imaging techniques). Ultrasonic tissue characterization with integrated backscatter has been used to assess myocardial texture, but is non-specific.[10,11] Finally, two-dimensional deformation imaging is useful for the assessment of LV longitudinal dysfunction, which is frequently impaired in most forms of RCM[12] (see Section Main forms of RCM and value of imaging techniques), and may help differentiating RCM form CP.[13]

Cardiovascular magnetic resonance

Cardiovascular magnetic resonance (CMR) imaging can contribute importantly to the diagnosis of RCM and the differential diagnosis from pericardial constriction.[14] The CMR methods most commonly used for the assessment of RCM include static (black blood) images, cine and contrast enhanced imaging as well as parametric mapping.

Static images are used to delineate cardiac, pericardial and vascular morphology. T1 and T2 weighted black blood images are sensitive to different tissue characteristics and provide complementary information. T1 weighted images show high signal from fat, as may for example be seen in Fabry's disease, while T2 weighted short tau inversion recovery (STIR) images show high signal in myocardial oedema, for example in acute sarcoidosis.

CMR allows accurate volumetric assessment of the heart and can accurately measure chamber size and function.[15] Typical cine CMR images are averaged over several heart beats to maximize image quality and temporal resolution, but real-time imaging can also be performed to demonstrate the typical septal shift during respiratory manoeuvers and identify restrictive physiology.[16] Velocity encoded CMR in standardized imaging planes perpendicular to the atrio-ventricular (AV) heart valves is used to demonstrate the typical restrictive filling patterns of accentuated early filling and absent or reduced late filling.[17]

A unique feature of CMR of relevance to the imaging of RCM is tissue characterization with late gadolinium enhancement (LGE). Following intravenous administration gadolinium-based contrast agents are retained preferentially in tissues with an expanded extracellular space, such as fibrosis, scar or infiltration. Characteristic patterns of contrast enhancement can be observed in several of the RCMs, contributing to the differential diagnosis of Fabry disease, amyloidosis, EMF, and sarcoidosis (*Figure* 2). In many of these conditions, the presence of LGE also has important prognostic

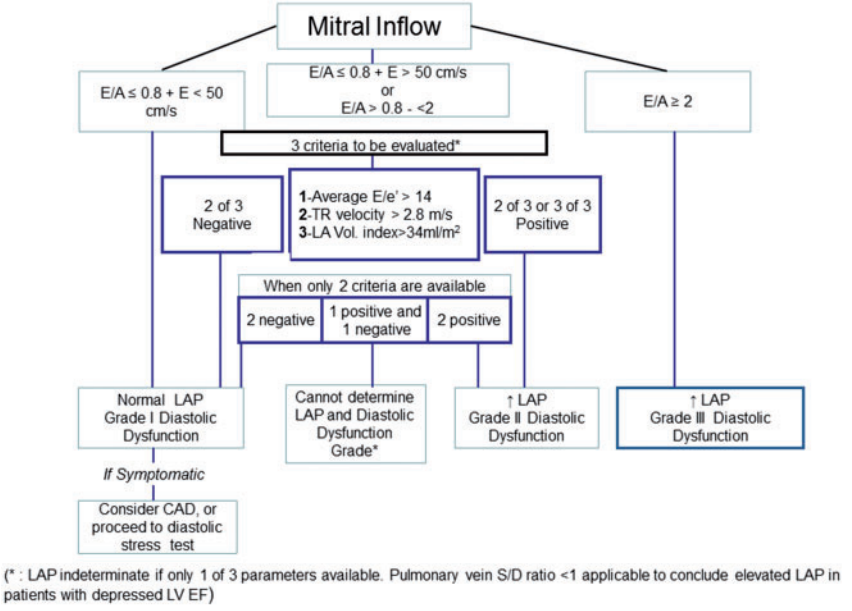

Figure 1 ASE—EACVI criteria for grading LV diastolic function in patients with depressed LVEF and patients with myocardial disease and normal LVEF after consideration of clinical and other two-dimensional data (from reference 8 with permission).

relevance.[18–20] Finally, parametric mapping methods have increasing applications in RCM and allow quantitative measurement of tissue characteristics. T2*-weighted CMR is now the method of choice to detect and quantify myocardial iron content in iron deposition cardiomyopathy and to guide appropriate therapy.[21] A low myocardial T2* value in this context is currently considered the most powerful marker of adverse outcome.[22] More recently, T1 mapping has been used to quantify the extent of myocardial inflammation and fibrosis. Native T1 relaxation times, as measured with T1 mapping without the need for contrast agent administration, are altered in several conditions including amyloidosis and may have incremental value over LGE imaging.[23] The combination of native and post-contrast T1 mapping allows an estimation of the myocardial extracellular volume (ECV) fraction, which in amyloidosis can even show differences in subtypes of the disease.[24] T1 mapping may also be useful in iron overload instead of the more established T2* mapping.[25]

Cardiac computed tomography

The key advantage of computed tomography (CT) is its high-spatial resolution and the anatomical detail it provides. However the associated radiation exposure largely limits this modality to static imaging, precluding dynamic analyses of LV haemodynamics, filling, or relaxation. Nevertheless CT is well suited to identifying the anatomic features of impaired cardiac filling that characterize RCM. These include dilatation of the atria, coronary sinus and inferior vena cava and the presence of pulmonary congestion and pleural effusions. These features are also observed in a range of other conditions and the predominant role of CT with respect to RCM is in the exclusion of these alternative diagnoses. In particular, CT is well suited to detecting the thickening and calcification of the pericardium most commonly associated with CP.[26] Similarly CT allows assessment of extra-cardiac involvement in systemic conditions such as sarcoidosis (e.g. pulmonary nodules, pulmonary fibrosis, and lymphadenopathy) or amyloidosis (e.g. inhomogeneous hepatomegaly, diffuse lung parenchymal involvement, small kidneys) further aiding in the differential diagnosis.

When other imaging modalities are not available, CT may be useful in evaluation of patients with RCM, owing to its ability to measure LV wall thickness and mass, detect regional wall thickening,[27] regions of replacement fibrosis,[27,28] and measure myocardial ECV fraction by equilibrium contrast-enhanced CT to assess diffuse fibrosis.[29] These advances may increase the clinical utility of CT in the future clinical assessment of patients with RCM, particularly when echocardiography and CMR are non-diagnostic or contraindicated.

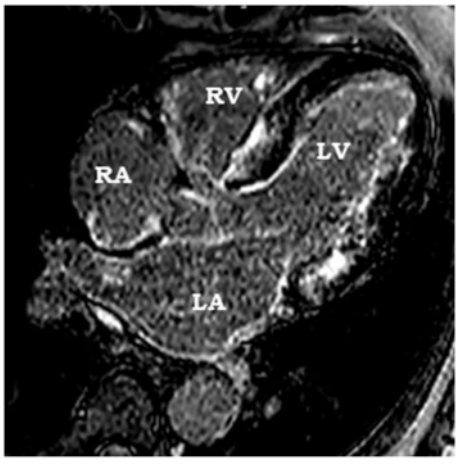

Figure 2 Seventy-four year-old patient presenting with breathlessness. Cine CMR showed global LV hypertrophy, impaired longitudinal LV shortening, and dilated atria. Late gadolinium enhanced CMR in the figure showed diffuse endocardial enhancement consistent with infiltrative disease. Subsequently, the patient was found to have amyloidosis. LV, left ventricle; RV, right ventricle; LA, left atrium; RA, right atrium.

Nuclear imaging

Nuclear imaging modalities have a potential clinical role in two forms of RCM: amyloidosis and sarcoidosis (see Sections Cardiac amyloidosis and Non familial/non-genetic RCM: inflammatory cardiomyopathies with a restrictive haemodynamic component). Nuclear imaging modalities have the advantage of specific targeted molecular imaging. Positron emission tomography (PET) has the technical advantages of high-spatial resolution, robust built-in attenuation correction, quantitative analysis, and low-patient radiation exposure, whereas single photon emission computed tomography (SPECT) has the advantage of a robust, cheaper, and well-validated camera system.

There are increasing data on the role of nuclear tracers with SPECT and more recently with PET for early identification and differential diagnosis of CA, particularly transthyretin-related amyloidosis (ATTR)

Radiolabelled SPECT phosphate derivatives, initially developed as bone-seeking tracers, were noted to localize to amyloid deposits using [99mTc]-diphosphanate.[30] In clinical practice, the most used SPECT tracers are: 99mTc-DPD mainly in Europe and Asia and 99mTc-PYP in the USA. Their main advantage is avid uptake by ATTR and minimal uptake with the light-chain (AL) amyloidosis subtype, providing one of the best non-invasive ways to differentiate these subtypes of CA.[31,32]

The imaging technique is simple. Briefly, after administering 740 MBq of 99mTc-DPD, or [99mTc]-HDP,[32,33] or of 99mTc-PYP[34] intravenously, a whole-body scan is performed 3 h or 1 h later (anterior and posterior projections). If there is active uptake in the heart, chest SPECT is performed. The analysis is performed by semi-quantitative visual scoring of the cardiac as compared to the bone uptake (scores from 0 to 3) and by computing the ratio, after correction for background counts, of the mean counts in the heart region over the mean counts in the contralateral chest (H/CL ratio).

Other nuclear imaging approaches have been recently proposed for the diagnosis and prognostic stratification of patients with suspected amyloidosis.[31] PET imaging using new amyloid tracers like the [11C]-labelled Pittsburgh Compound B (PiB) or [18F]-florbetapir is promising and under early clinical investigation. The use of neuronal imaging by [123-I]-MIBG SPECT has been suggested for early recognition of cardiac involvement and prognostic stratification of individuals with TTR mutation.[34]

The inflammatory nature of cardiac sarcoidosis (CS) renders PET useful for its diagnosis, as [^{18}F]FDG accumulates in inflammatory cells

in the heart. FDG is preferred in combination with a perfusion tracer to improve specificity due to better match/mismatch pattern recognition. Unlike in CMR, there is no distinct pattern of FDG uptake that is pathognomonic for CS, though focal or focal on diffuse uptake is suggestive of the disorder.[35] At present, [^{18}F]FDG-PET appears to be more sensitive but less specific than CMR[36] and its use seems most appropriate in patients who have contraindications to CMR, inconclusive findings on CMR or where CMR is not available also to monitor response to therapy. The development of FDG PET/MR techniques offers the ability to assess LV wall function, the pattern of myocardial injury and disease activity in a single scan.[37] (*Figure 3*).

In summary, several imaging techniques are available in the evaluation of RCM, all of which have both advantages and limitations. Table 2 summarizes the value of different imaging modalities in various forms of RCM. Although non-invasive techniques are sufficient in most cases, final histologic diagnosis may sometimes be necessary, and may be obtained by biopsies specimens from the heart [endomyocardial biopsies (EMB)] or other organs. Figure 4 illustrates by histology and immunohistology different disease entities of RCM which will be discussed in the following chapters.

Main forms of RCM and value of imaging techniques

Apparently idiopathic RCM

Apparently idiopathic RCM may be caused by mutations in sarcomeric disease genes and may even coexist with HCM in the same

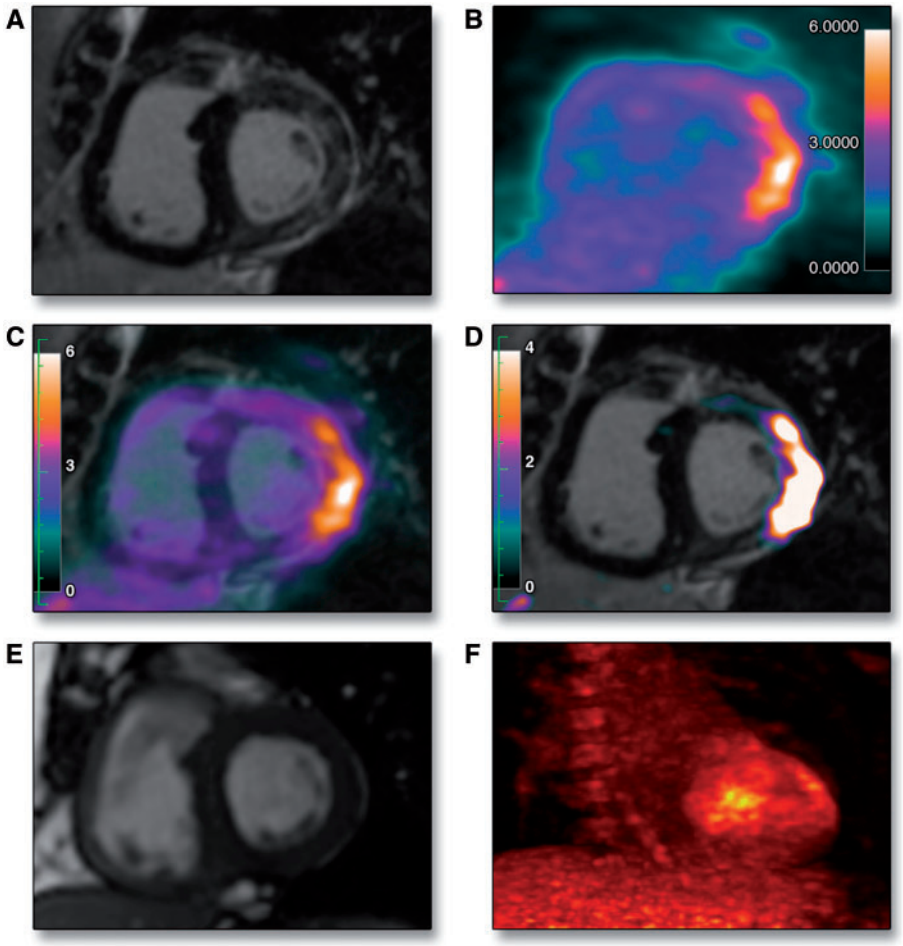

Figure 3 Patient with acute myocardial sarcoidosis (from reference 37 with permission). Patient (62-year-old male) followed for histologically proven pulmonary sarcoidosis treated by steroids for 10 years presented with symptoms of acute breathlessness. Cardiac involvement was suspected. LGE-CMR (*A*) images showed patchy LGE of the lateral wall. Matched FDG-PET (*B*) and fused FDG-PET/MR (*C* and *D*) images obtained in short-axis view showed intense uptake in exactly the same territory as the pattern of injury on CMR (maximum standardized uptake value of LGE territory/blood pool uptake ratio = 2.7). A two-chamber cine CMR (*E*) sequence showed mild hypokinesis of the lateral wall and mild overall LV systolic impairment (LV ejection fraction = 52%). Maximum intensity projection FDG-PET (*F*) cine view confirmed abnormal myocardial uptake without evidence of increased activity outside of the heart.

Table 2 Value of different imaging modalities in various forms of RCM

	TTE	TDI and strain imaging	CMR	Nuclear imaging	Cardiac CT	PET
Apparently idiopathic RCM	+++	++	++	0	+	0
Cardiac amyloidosis	+++	+++	+++	+++	+	+
Other causes of familial/genetic RCM						
Haemochromatosis	+++	+	+++	+	0	0
Fabry cardiomyopathy	++	++	+++	0	0	0
Glycogen storage disease	++	++	++	+	0	0
Pseudoxanthoma elasticum	++	+	++	+	0	0
Inflammatory CM with a restrictive component						
Cardiac sarcoidosis	+	0	++	++	+	+++
Systemic sclerosis	++	++	++	+	0	0
Radiation therapy and cancer drug therapy induced RCM						
Cardiac toxicity of radiation therapy	++	+	++	+	0	0
Cancer drug induced RCM	+++	++	++	0	0	0
Endomyocardial RCMs						
Endomyocardial fibrosis	+++	+	+++	0	0	0
Hypereosinophilic syndrome	+++	+	+++	0	0	0
Carcinoid heart disease	+++	0	++	0	0	0
Drug-induced endomyocardial fibrosis	+++	0	++	0	0	0
Differential diagnosis with CP	+++	++	++	0	+++	0

RCM, restrictive cardiomyopathy; TDI, tissue Doppler imaging; CMR, cardiovascular magnetic resonance; PET, positron emission tomography; CT, computed tomography; TTE, transthoracic echocardiography.

family[38–40] and may require EMB (to exclude CA), family screening, and genetic investigations. Most affected individuals have severe signs and symptoms of heart failure. Several studies have reported that 66–100% die or receive a cardiac transplant within a few years of diagnosis.

The echocardiographic diagnosis is one of restrictive physiology and mostly preserved LV ejection fraction. Typically, idiopathic RCM is characterized by diastolic dysfunction with apparently preserved systolic function, dilated atria, and the absence of ventricular hypertrophy or dilatation (*Figure 5* and see Supplementary data online, *Videos S1 and S2*). Longitudinal function may be decreased; the right ventricle may be involved but there is no 'pathognomonic' echocardiographic pattern of apparently idiopathic RCM. CMR with LGE may facilitate the diagnosis of infiltrative myocardial disease, and is thus particularly useful for ruling out a particular cause of RCM.[41]

Cardiac amyloidosis

CA is one of the most frequent causes of RCM and may be genetic/familial (ATTR) or non-genetic non-familial (AL/prealbumin, senile).

The diagnosis requires awareness, expertise and a high level of clinical suspicion, with integration between clinical, electrocardiographic, and echocardiographic data. The 'mismatch' between the presence of LV hypertrophy (LVH) in echocardiography and its absence on the ECG (no LVH, absolute, or relative low-voltage QRS) is suggestive of CA and is often the first disease 'red flag'.[42,43] Typical echocardiographic findings in CA patients include (*Figure 6A*) a non-dilated LV with moderate concentric LVH and a 'granular sparkling' appearance of the myocardial texture, valvular thickening (mainly the AV valves), biatrial dilatation, right ventricular free wall hypertrophy, inter atrial septum infiltration (loss of physiological echo drop-out), and mild pericardial effusion.[44] In the early stages of the disease, CA may present as asymmetrical septal hypertrophy, sometimes with LV outflow tract obstruction and can then be wrongly diagnosed as HCM. The presence of intra-atrial thrombus also seems to be relatively frequent in patients with CA, even in sinus rhythm.[45]

Patients often show (*Figure 6B*) advanced diastolic dysfunction (Grade II or III) and increased LV filling pressures. The classical transmitral restrictive pattern may only be seen at advanced disease stages. The typical tissue Doppler imaging (TDI) pattern of CA, with low systolic (s') and diastolic (e', a') myocardial velocities. Of note, E/e' ratio is usually abnormally increased even in the presence of LV abnormal relaxation pattern (diastolic dysfunction Grade I).[46]

LV systolic dysfunction is also a common finding in this disease. In early stages, despite preserved LV ejection fraction, longitudinal function is abnormal (abnormal long axis systolic velocities (s') and strain) (*Figure 7A*) as well as myocardial contraction fraction, a recently described systolic parameter.[47]

Two-dimensional speckle-tracing echocardiography (2D-STE) is important, as many systolic strain parameters (longitudinal, circumferential, radial) are abnormal in CA, particularly in the longitudinal axis, typically with prominent involvement of LV basal segments and apical sparing[48] (*Figure 7B*), reflecting the predominant deposition of amyloid in basal segments. The combination of a prominent reduction of longitudinal strain in LV basal segments with increased E/e' ratio suggests CA in early stages.[49]

Multiple echocardiographic parameters have been associated with adverse outcomes in CA, including M- mode and two-dimensional data (maximal wall thickness, LV fractional shortening and LV ejection fraction, right ventricle dilatation), blood pool Doppler data (restrictive filling pattern, myocardial performance index, Tissue Doppler

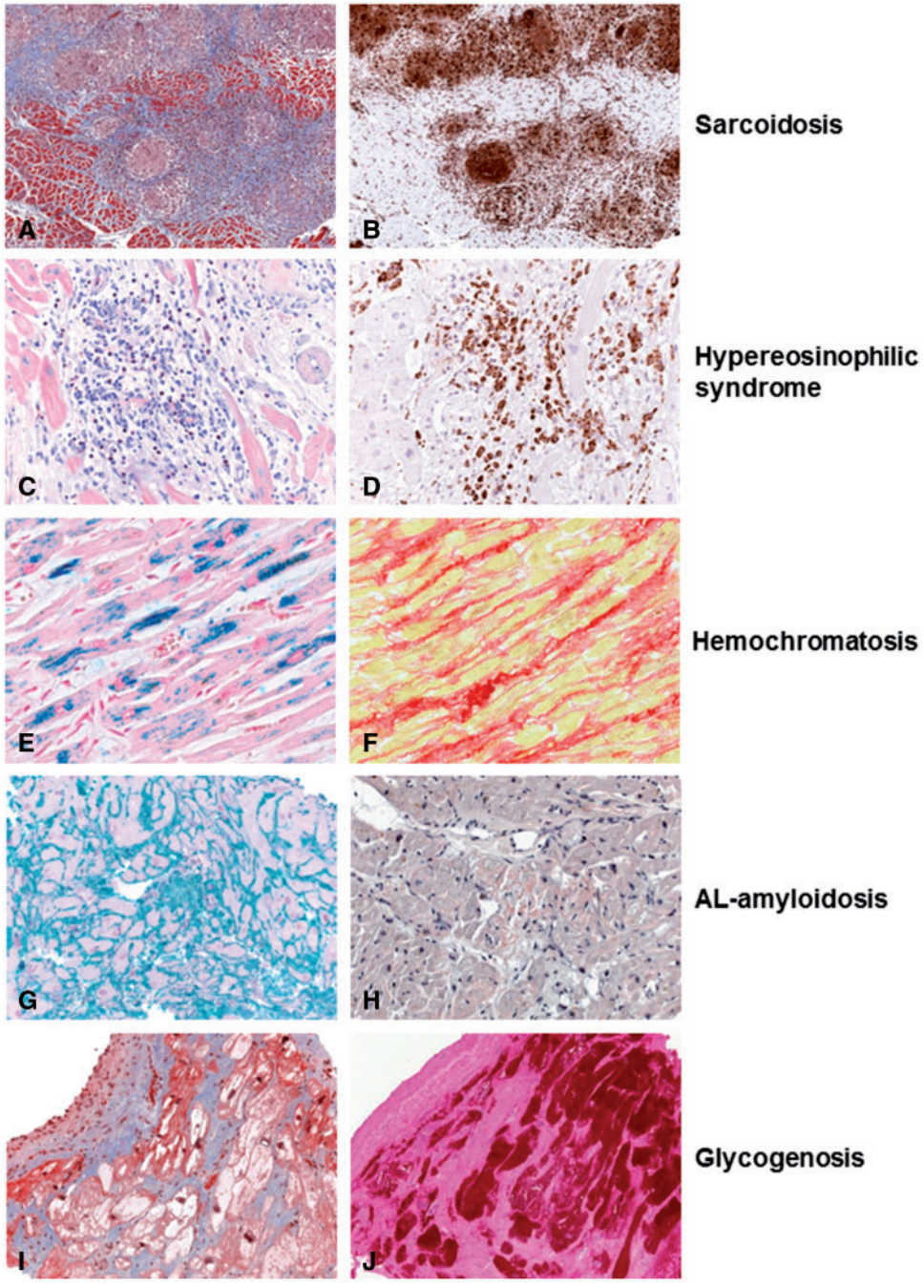

Figure 4 Imaging of RCM at the cellular level. Different disease entities of RCM are visualized by histology and immunohistology. Sarcoidosis with typical granulomas, fibrosis (blue tissue) (*A*, Masson trichrome stain), and numerous CD68+ macrophages and giant cells (*B*, immunohistochemistry). Hypereosinophilic syndrome with myocyte necrosis, eosinophilic granulocytes, (*C*, Giemsa stain) and CD68 + macrophages (*D*, immunohistochemistry). Storage diseases: haemochromatosis with iron containing myocytes (*E*, Prussian blue) and fibrosis (*F*, Sirius red). AL-amyloidosis (*G*, AL-amyloid immunohistochemistry (green), *H*, Kongo red). Glycogenosis with hypertrophic, vacuolated myocytes, and fibrosis (*I*, Masson trichrome stain) and large amounts of glycogen (*J*, PAS stain (red)) (A and B: x100; C–J: x200).

derived data (myocardial velocities, long axis velocity gradient, peak longitudinal systolic basal antero-septal strain > -7.5%),[50] and 2D-STE parameters [global longitudinal strain (GLS), mid-septum systolic longitudinal strain, apical LS< -14.5%].[51,52]

CMR is often used after CA is suspected by echocardiography to confirm or refute the diagnosis, and in experienced hands represents a powerful tool with important diagnostic and prognostic implications. Cine images may demonstrate typical anatomical features like

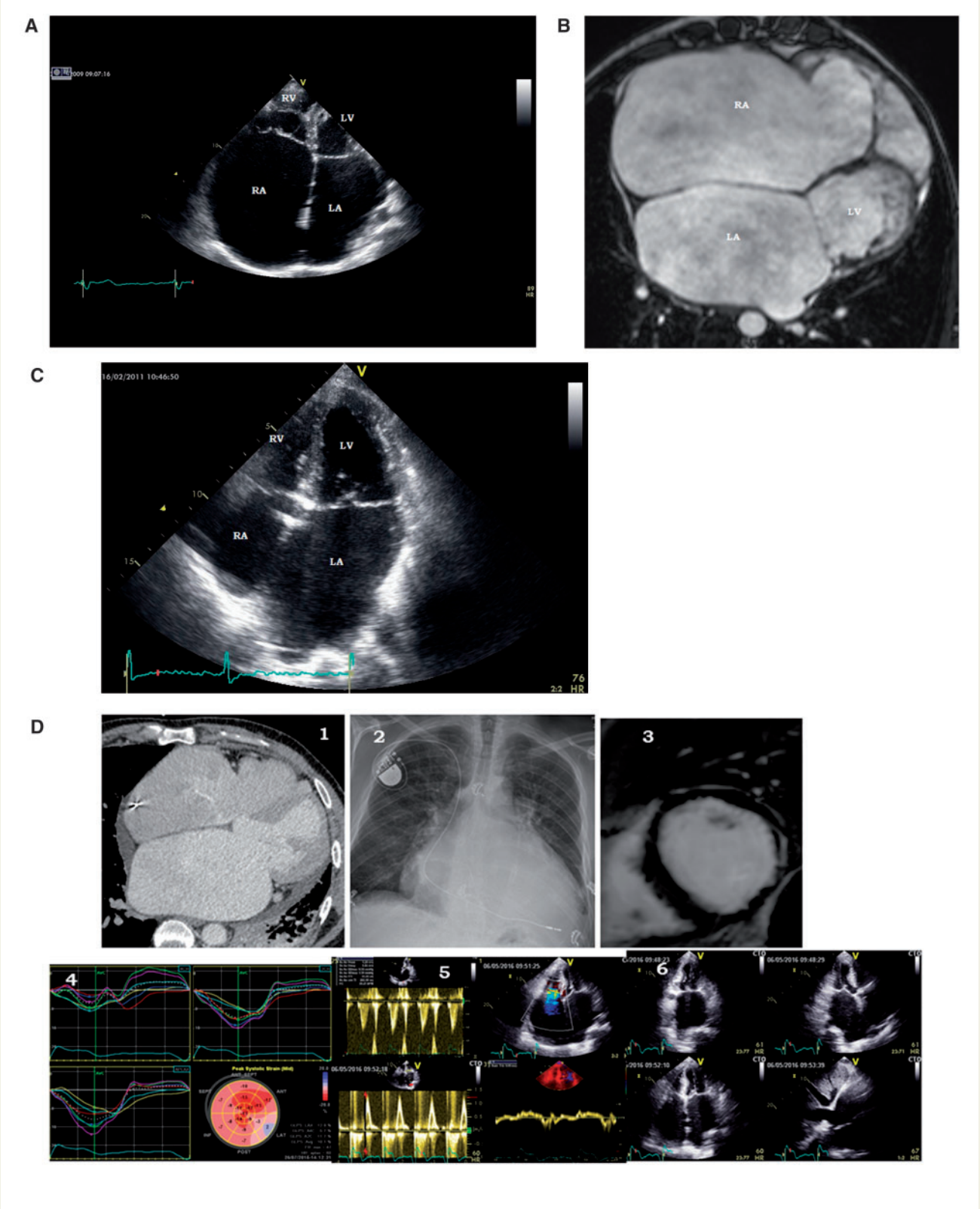

Figure 5 Multimodality imaging findings in three patients with apparently idiopathic RCM. (*A*) (TTE) and (*B*) (CMR) Impressive dilatation of both atria predominating on the right cavities, contrasting with small LV and RV cavities (Supplementary data online, *Video S1*). (*C*) More classical form of idiopathic RCM with normal ventricular systolic function and severe atrial dilatation. RA, right atrium; RV, right ventricle; LV, left ventricle; LA, left atrium (Supplementary data online, *Video S2*). (*D*) Multimodality imaging in a severe RCM. Patient in atrial fibrillation and a pace maker for severe AV block. Huge atria that can be seen on the CT, (1) the chest X-ray, (2) and the Echocardiography. (6) There is a severe tricuspid regurgitation (5) and a severe alteration of the longitudinal systolic and diastolic function as shown by the tissue Doppler (5) and the strain data. (4) Extensive circumferential subendocardial late gadolinium enhancement is observed by CMR (3).

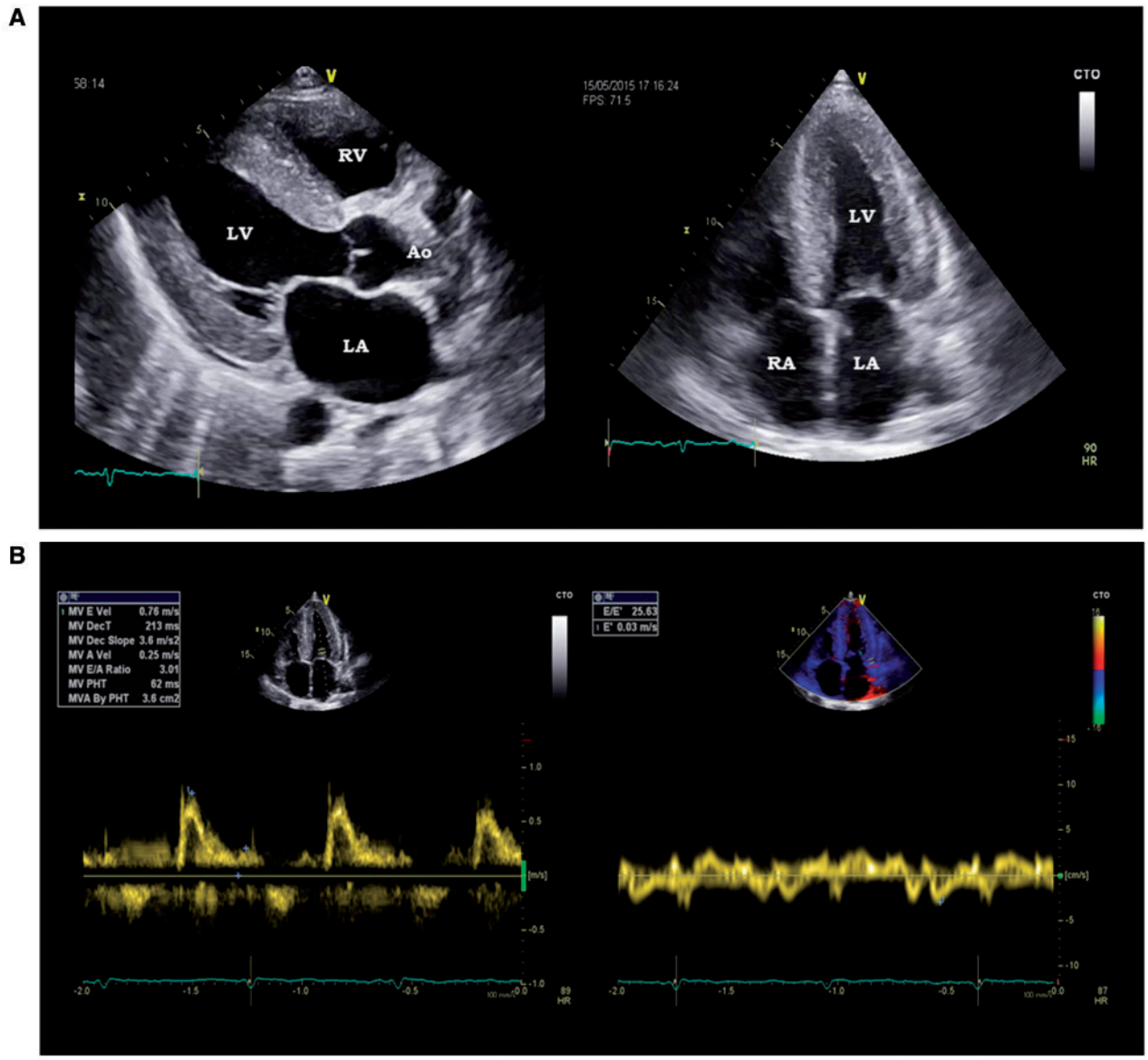

Figure 6 (*A*) Two-dimensional echocardiography in a 52-year-old male with CA, AL type, associated with plasma cell dyscrasia: non-dilated LV with moderate concentric LVH with 'granular sparkling' appearance, mitral valve thickening, mild to moderate biatrial dilatation, inter atrial septum infiltration (loss of physiological echo drop-out) and mild pericardial effusion. RA, right atrium; RV, right ventricle; LV, left ventricle; LA, left atrium; Ao, aorta. (*B*) Diastolic function in the same patient: E/A $\gg$1 (PWD transmitral inflow), low-systolic and diastolic myocardial velocities (TDI), E/e' =25, reflecting high-LV filling pressures.

thickened LV wall, biatrial enlargement, reduced long-axis shortening, and pleural or pericardial effusion. The presence of amyloid protein in the myocardial interstitium is associated with abnormal gadolinium-chelate contrast kinetics and characteristic patterns of contrast distribution. LGE images typically show circumferential subendocardial contrast enhancement or bilateral septal subendocardial LGE with dark mid-wall (zebra pattern) (*Figure 8A*),[53,54] but other patterns of enhancement have also been described. In atypical cases, other differential diagnoses should be considered such as HCM or Fabry's disease. Cardiac involvement can extend to the right ventricle and atrial walls, as potentially detected by LGE. The extent of myocardial LGE correlates with New York Heart Association functional class, LV wall thickness, lower ECG voltage, and cardiac biomarkers (troponins, brain natriuretic peptide).[55] With more advanced disease, amyloid infiltration may be transmural with corresponding global enhancement on LGE images, which is an independent predictor of poorer outcomes, over stroke volume and pro-NT brain natriuretic peptide.[19]

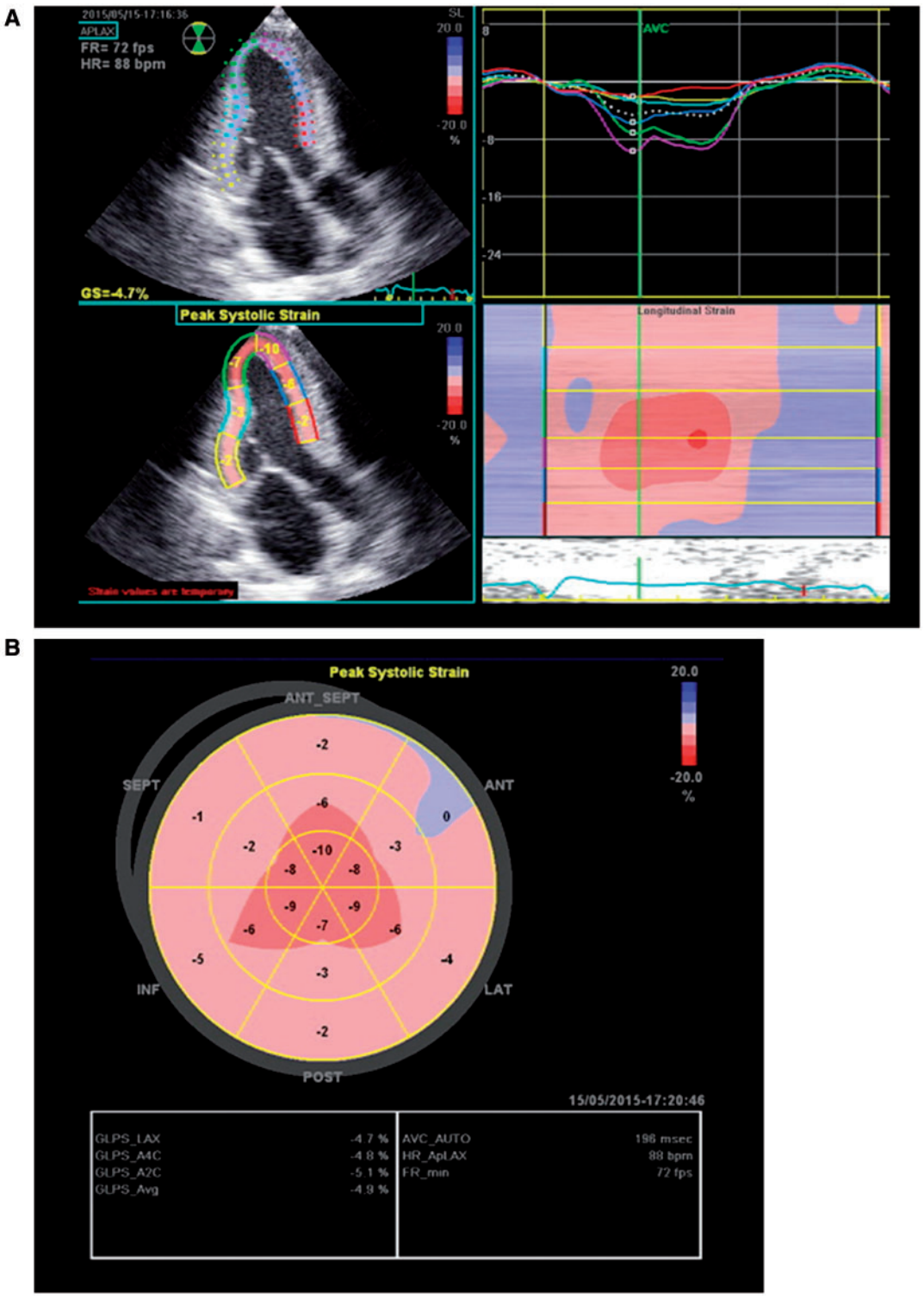

Figure 7 (*A*) Two-dimensional-STE apical longitudinal view in systemic AL amyloidosis: severely abnormal longitudinal strain, particularly in the basal and medial LV segments. (*B*) Systemic AL amyloidosis, multiple myeloma: 2D-STE, relative apical sparing, typical of CA. Note the abnormal GLS (-4.9%).

Amyloid deposits increase the longitudinal relaxation time (T1) magnetic property of the heart. Thus, myocardial non-contrast T1 values are longer in CA than in controls, a finding with higher sensitivity for detecting early subclinical cardiac involvement than LGE.[23] ECV estimation from pre- and post-contrast T1 mapping has been used to quantify interstitial amyloid deposition which appears to be more extensive in transthyretin amyloidosis (TTR) than in immunoglobulin AL.[56] The addition of parametric mapping to standard CMR images is promising to be a powerful and quantitative diagnostic tool that also allows differential diagnosis from other diseases with similar phenotypic expression.

Scintigraphy employs molecular-targeted radiolabelled compounds to detect systemic and organ-specific amyloid deposits. Scintigraphy is a valuable alternative to CMR particularly for patients with ATTR amyloidosis due to its very high sensitivity. Scintigraphy may also be used following an inconclusive CMR study, or for phenotyping CA (ATTR vs. AL) or in the differential diagnosis with sarcomeric HCM.[57,58] The [99mTc]-labelled bisphosphonate compounds pyrophosphate (PYP)[58] and 3,3-diphosphono-1,2-propanodicarboxylic acid (DPD),[59] and hydroxydiphosphonate (HDP)[33] (which are routinely used as bone scintigraphy agents) bind through unknown mechanisms to amyloid protein. All have proven very sensitive for detecting

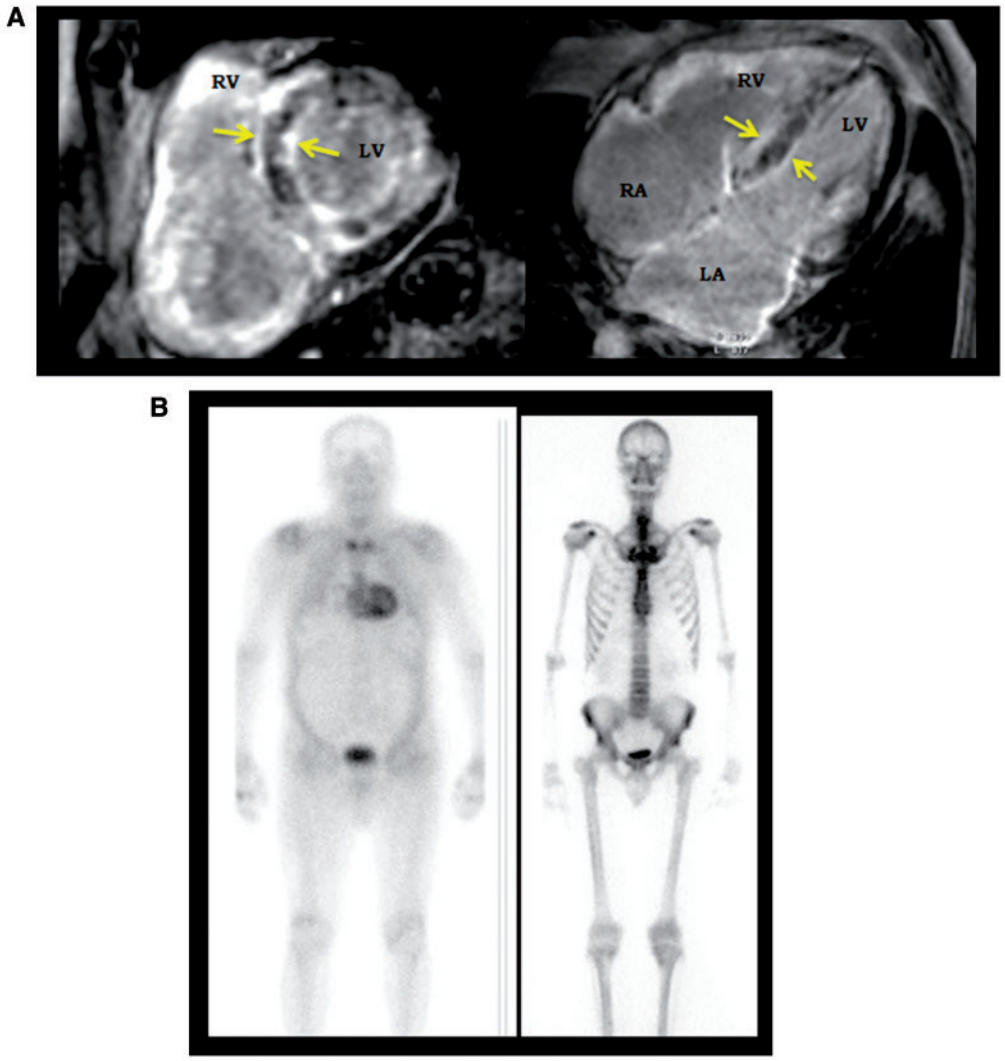

Figure 8 (*A*) CMR in a 79-year-old patient with CA showing mild septal hypertrophy (16 mm), biatrial enlargement, and diffuse patchy uptake of gadolinium throughout the mid-ventricular and basal segments of the septal, anterior, and inferior wall with sparing of the apicolateral wall. (Note small areas of bilateral subendocardial LGE in the septal wall characteristic of CA (arrows) and LGE in the right ventricular free wall and the left atrium). RA, right atrium; RV, right ventricle; LV, left ventricle; LA, left atrium. (*B*) Late-phase planar 99mTc-DPD-scintigraphy (anterior views) in a patient with ATTR amyloidosis (A) and a normal control (B). Note intense cardiac uptake in (A) demonstrating CA. Moreover, increased soft tissue uptake particularly in the shoulder region and the abdominal wall with obscuring of bone uptake can be observed as a typical pattern of ATTR amyloidosis.

cardiac involvement in ATTR amyloidosis with reported sensitivities up to 100% on late phase planar scintigraphy. Typical uptake patterns besides cardiac uptake in ATTR amyloidosis include increased soft tissue uptake (mainly muscular uptake in the gluteal, shoulder, chest, and abdominal wall regions) with obscuring of bone uptake (*Figure 8B*). However, in AL amyloidosis, cardiac uptake is found in less than half of patients and is generally less intense (likely due to the lower concentration of calcium-containing products in AL amyloid). Additionally, AL patients have generally no muscular [99mTc]-DPD or [99mTc]-HDP uptake while visceral uptake (liver, spleen) may be more common.

Even if there are not yet large comparative studies, the diagnostic performance of nuclear imaging for CA is established. In general, [99mTc]-DPD can differentiate subtypes[60] and can be more sensitive than CMR[33] or echocardiography in diagnosing early disease being an independent prognostic marker.[61] In a recent study by Bokhari *et al.*[58] using 99mTc-PYP, while patients with AL had some uptake, the visual score was significantly less than in patients with ATTR, allowing the differentiation between ATTR and AL amyloidosis with 97% sensitivity and 100% specificity.

Hence, whole body planar DPD and HDP scintigraphy may help to phenotype CA particularly through differentiating ATTR from AL amyloidosis (or from sarcomeric HCM, where no DPD uptake is seen), which often have overlapping imaging features on echocardiography and CMR, but very distinct clinical course and prognosis. Moreover, a recent comparison of [99mTc]-DPD scintigraphy and LGE showed that despite a general good agreement between both techniques, LGE may sometimes underestimate cardiac amyloid burden.[33] Finally, myocardial tracer uptake on scintigraphy is correlated with disease severity (measured by circulating troponin and LV wall mass), and has been shown to be a powerful prognostic determinant of outcome in ATTR CA.[32,61]

Recent investigations found that bone scintigraphy enables the diagnosis of cardiac ATTR amyloidosis to be made reliably without the need for histology in patients who do not have a monoclonal gammapathy.[62] The algorithm proposed (*Figure 9*) that cardiac ATTR amyloidosis can be reliably diagnosed in the absence of histology provided an echocardiogram or CMR is suggestive of amyloidosis, cardiac uptake is present on scintigraphy and there is absence of a detectable monoclonal gammapathy. Histological confirmation and typing of amyloid should be sought in all cases of suspected CA in which these criteria are not met.

In summary, all these imaging techniques are useful and give additional information, including echocardiography, nuclear techniques and CMR (Table 3),[63] but also EMB and genetic testing, to differentiate ATTR mutant from wild type. Figure 10 illustrates the value of multimodality imaging in a patient with CA.

Other causes of familial/genetic RCM

Haemochromatosis

Iron overload cardiomyopathy (IOC) results from iron accumulation in the myocardium mainly because of genetic disorders of iron metabolism (primary haemochromatosis) or multiple transfusions (such as in thalassaemia or myelodysplastic syndromes).

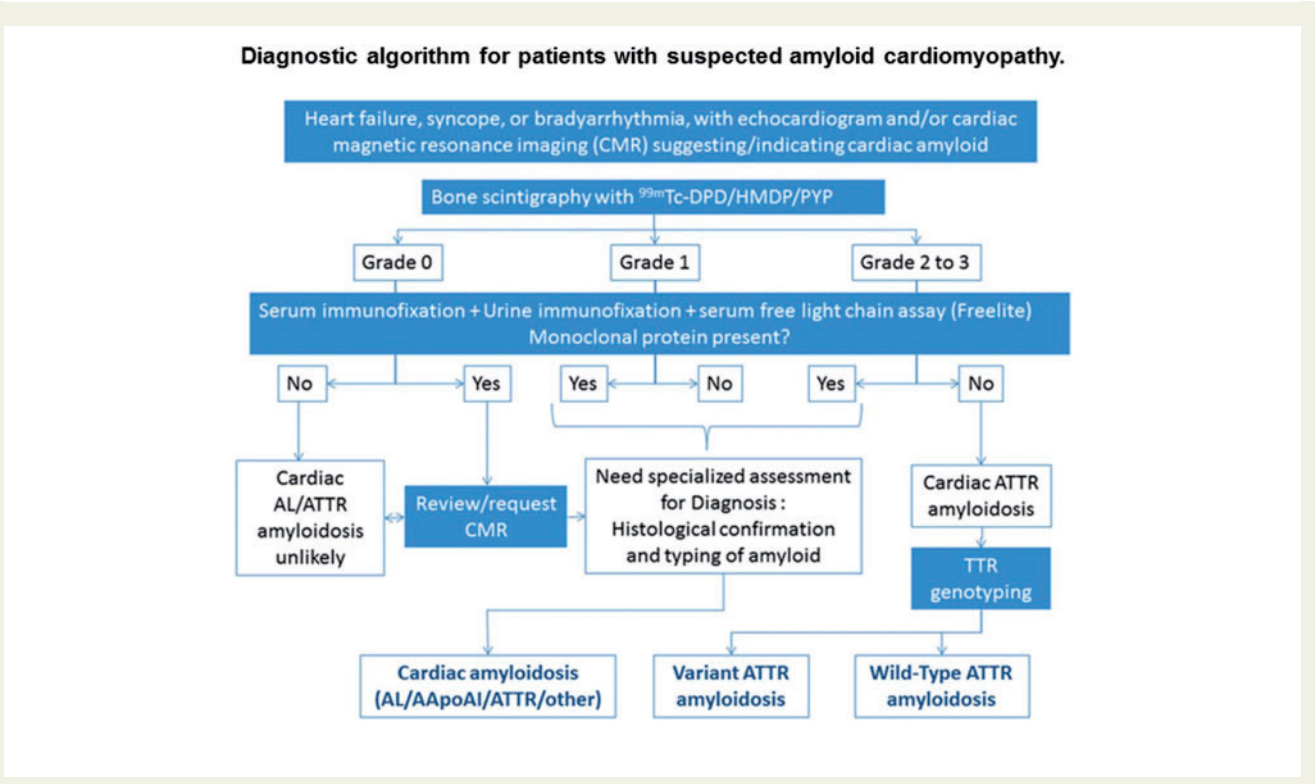

Figure 9 Diagnostic algorithm for patients with suspected amyloid cardiomyopathy (from reference 62 with permission). AApoA1, apolipoprotein A-I; DPD, 3,3-diphosphono-1,2-propanodicarboxylic acid; HDMP, hydroxymethylene diphosphonate; PYP, pyrophosphate.

In the early stages, myocardial iron overload (MIO) causes diastolic LV dysfunction.[64] If no effective iron chelation is instituted in time, the majority of patients develops LV dilatation and reduced LV ejection fraction (EF) (dilated phenotype).[65] In a minority of cases with severe MIO, restrictive LV dysfunction can lead to pulmonary hypertension, right ventricular dilatation, and right-sided heart failure with preserved LVEF (restrictive phenotype).[66]

Echocardiography is a useful modality in the follow-up of iron-loaded patients. A pseudonormalized pattern of transmitral inflow is frequently encountered and may be unmasked by tissue Doppler.[67] LV diastolic dysfunction and reduced EF may both be masked by an anaemia-induced high-cardiac output state in haematologic patients. There are few data relating diastolic function to outcome in haemochromatosis.[68]

However, due to the lower accuracy in quantifying biventricular systolic function and the lack of parameters able to predict MIO reliably, echocardiography is only the second-line imaging method after CMR.[69,70]

The method of choice for assessing IOC is CMR, which allows tissue characterization including quantification of MIO. The paramagnetic effect of iron-loaded myocardium affects T1, T2, and T2* relaxation times which can be used to calculate MIO. The best validated method for quantifying MIO is T2* mapping. T2* values correlate closely with hepatic and myocardial iron content and correlate better with LV dilatation and LV dysfunction than serum ferritin or liver iron concentration. A T2* value of < 20 ms at 1.5 Tesla, typically measured in the interventricular septum, is used as a conservative cut-off for segmental and global heart iron overload and patients with the lowest T2* values have the highest risk of developing arrhythmia and heart failure. T2* CMR has revolutionized IOC management with the death rate in patients with thalassaemia falling dramatically in countries where T2* CMR has been adopted. In the assessment of IOC, the first cardiac T2* assessment should be performed as early as possible and the effectiveness of iron chelation[71] and reversal of MIO can be reliably guided by follow up scans.[72] A multislice approach can detect the uneven distribution of MIO, allowing early identification of patients at risk of cardiac complications.[73]

T2* is dependent on field strength and sensitive to field inhomogeneity. T2 and T1 mapping techniques offer some advantages over T2* and have been compared with standard methods, with initial studies showing close correlation with T2*.

In patients where the diagnosis is unclear, a multiparametric CMR approach that evaluates cardiac function, myocardial fibrosis and oedema may allow further clarification of the underlying mechanisms leading to the LV dysfunction.[74]

In summary, cardiac involvement is frequent in haemochromatosis. CMR is the main imaging technique for diagnosis and follow-up of cardiac haemochromatosis, allowing both reliable measurement of LV and RV dimension and function and tissue characterization including quantification of MIO.

Fabry cardiomyopathy

Cardiac involvement is very common and is the most frequent cause of death not only in haemizygote males but also in female heterozygote carriers with α-Gal A deficiency, with a reduction of life expectancy of approximately 20 and 15 years respectively.[75] The heart may be the only organ affected in the classic phenotype of Fabry disease, and this is designated the 'cardiac variant'.[76]

Cardiovascular manifestations include renovascular and systemic hypertension, aortic root dilatation, mitral prolapse, and congestive heart failure.[77] Fabry cardiomyopathy mainly consists of progressive LVH, which may cause substantial morbidity and contribute to the reduced life expectancy of affected patients, both male and female.[78,79]

LVH is a hallmark of Fabry cardiomyopathy.[80] In patient populations with HCM, the prevalence of Fabry disease ranges from 0 to 12%, depending on the patient selection criteria used, but is close to 1% in the largest series.[81] LVH is generally symmetrical, although asymmetric septal hypertrophy has been described, and the condition can mimic the phenotypical and clinical features of HCM, including obstructive HCM.[82] Typically, the echocardiogram shows marked increases in wall thickness and ventricular dilatation later in the disease process. Valve leaflet thickening can be seen, and this produces valve impairment that usually does not require surgical treatment.[83]

Table 3 Multimodality imaging in the differential diagnosis between HCM and CA (from Cardim *et al.*[63])

Imaging data	HCM	Cardiac amyloidosis
Echo, CMR, cardiac CT		
LVH	Severe, asymmetric	Moderate, concentric, 'sparkling'
Left ventricular outflow tract obstruction	Frequent	Rare (may exist in early stages)
Pericardial effusion	Rare	Frequent
IAS hypertrophy	Rare	Frequent
Apical sparing	Rare	Frequent
CMR		
LGE	RV insertion points, intramural	Diffuse, subendocardial (global or segmental)
T_1 mapping	Under research	Work in progress; typical patterns
CNI		
^{99m}Tc-DPD uptake	No	Yes (TTR—senile and familial

CMR, cardiovascular magnetic resonance; HCM, hypertrophic cardiomyopathy; LVH, left ventricular hypertrophy; LGE, late gadolinium enhancement; TTR, transthyretin.

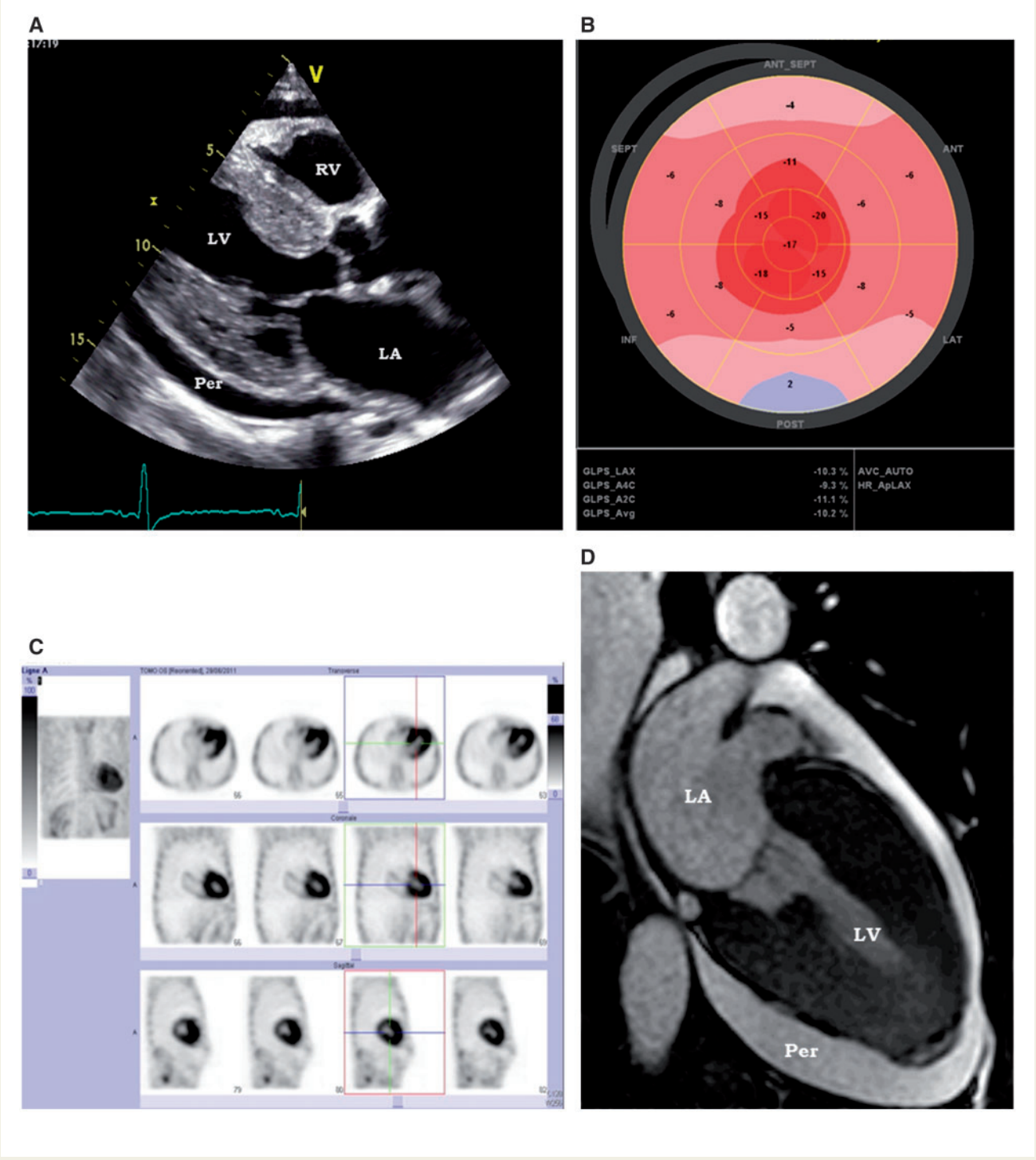

Figure 10 Multimodality imaging in a patient with familial TTR amyloidosis. (*A*) Two-dimensional echo long-axis view showing LV hypertrophy and pericardial effusion (Supplementary data online, *Video S3*). (*B*) Apical sparing by two-dimensional strain (Supplementary data online, *Video S4*). (*C*) Intense cardiac uptake on 99mTc scintigraphy. (*D*) CMR confirming LV hypertrophy and pericardial effusion (Supplementary data online, *Video S5*). RV, right ventricle; LV, left ventricle; LA, left atrium; Per, pericardial effusion.

Echocardiography using TDI can detect the first signs of myocardial damage in a patient with Fabry cardiomyopathy and normal cardiac wall thickness.[84] Furthermore, TDI studies have been shown to be useful in detecting cardiac involvement in female carriers with no systemic manifestations of Fabry disease. A reduction of TDI velocities may represent the first sign of initial intrinsic myocardial

impairment.[85] These reduced TDI velocities in mutation positives without LVH are consistent with the hypothesis that myocardial dysfunction precedes LVH.[86]

CMR with LGE may be useful in the non-invasive recognition of myocardial fibrosis, in the context of cardiac involvement of Fabry disease.[87] The LGE pattern of distribution helps in the differentiation between HCM and Fabry cardiomyopathy.[18] Patients with Fabry cardiomyopathy typically present with a pattern characterized by the involvement of the inferolateral basal or mid-basal segments.[87] Furthermore, the myocardial T2 relaxation time is prolonged in patients with Fabry disease compared with that in HCM patients, and its measurement could be complementary to the LGE technique. More recently, native T1 mapping was shown to be the most reliable technique to differentiate Fabry cardiomyopathy from all the other LVH phenocopies, by demonstrating a low native T1 value of the affected myocardium (whilst other LGE area of different disease would display a high native T1 values).[18] This important difference is due to the characteristic fatty nature of the infiltration in Fabry disease.

Finally, for most males with Fabry disease, the diagnosis can be made by measuring leucocyte and plasma α-Gal activity, while genetic testing is useful in patients with normal levels of enzyme activity.[18] A familial screening should be performed in patients with Fabry's disease (*Figure 11*).

In summary, cardiac involvement is frequent in Fabry disease and is associated with worse outcome. Imaging techniques, especially TDI and CMR, allow a comprehensive evaluation of cardiac involvement, even before morphological manifestations such as hypertrophy develop.

Glycogen storage disease

Glycogen storage disease is defined as the absence or deficiency of one of the enzymes responsible for making or breaking down glycogen in the body. The enzyme deficiency causes either abnormal tissue concentrations of glycogen or incorrectly or abnormally formed glycogen.[88,89] There are 11 different types of glycogen storage diseases causing different forms of heart failure. Most well-known are Danon and Pompe diseases.[80,90,91]

Danon cardiomyopathy is progressive and typically manifests a hypertrophic phenotype, with preserved LVEF and normal cavity dimensions early in the course of disease, and later progression to dilated features in 11–12% of men.[89] HCM is predominant in male patients, whereas an equal prevalence of hypertrophic and dilated cardiomyopathy is seen in female patients.[90]

Echocardiography demonstrates increased LV mass and wall thickness although LV systolic function is preserved. Taking into consideration the possible progress to cardiac failure, serial echocardiograms with attention to LV thickness and mass are important in the care of these patients.[91,92] Echocardiography is also the standard method to evaluate the cardiac response to enzyme replacement therapy.

Typical findings in CMR consist of significantly reduced LV global function and increase of LV end-diastolic and end-systolic volumes. Perfusion defects, mainly subendocardial, are visible in almost all segments on rest first-pass perfusion images. They may be obvious in the infero-septal segments and partly transmural in the lateral and anterior walls. LGE appears to be a rare finding in Pompe disease but when present, is seen in the subendocardium and in places transmurally in the anterior and lateral walls.[93,94]

A diagnosis of Danon disease is always confirmed by EMB results.

^{99}mTc-methoxyisobutylisonitrile myocardial imaging has also been employed as an imaging diagnostic test for glycogen storage disease, to detect myocardial damage as a non-invasive method. There has been a positive rate of detection of damage with G-MPI of 77.8%.[95]

Other storage/infiltrative diseases (Gaucher disease, mucopolysaccharidoses) may be rarely associated with cardiac involvement.[96,97]

Pseudoxanthoma elasticum

Pseudoxanthoma elasticum is a rare, inherited connective tissue disorder associated with coronary and peripheral arterial disease and accelerated atherosclerosis in medium sized arteries.[98] Cardiac involvement may start as a diffuse arteriopathy secondary to elastic fibre dysgenesis, involving the small intramural coronary vessels ('small-vessel disease') and it may reach the clinical presentation of congestive heart failure, even though—quite often—with normal epicardial vessels.[99]

Echocardiography detects impaired LV systolic and diastolic function.[100] Other imaging modalities—as functional tests—such as perfusion CMR or nuclear myocardial perfusion imaging, may be useful to demonstrate early coronary involvement and/or the direct consequences of ultrastructural defects of the elastic tissue of the heart. Increased awareness for silent ischaemia is recommended.[98,101]

An important study with arterial stiffness evaluation demonstrates the early detection of accelerated atherosclerosis and the impairment of the elastic properties of the aorta. A lower elasticity in large arteries, a higher cardiac output and a higher total vascular impedance were observed in patients with pseudoxanthoma elasticum with respect to the control group.[101]

Non-familial/non-genetic RCM: inflammatory cardiomyopathies with a restrictive haemodynamic component:

Cardiac sarcoidosis

Sarcoidosis is a multisystem inflammatory granulomatous disease of unknown origin. CS is frequently isolated.[102] Its diagnosis is difficult and has benefited from the use of multimodality imaging.

Although echocardiography is not the method of choice for the diagnosis of CS, it can offer very useful information in some cases.[103] An unexplained reduced LV ejection fraction < 40% in a patient with a histological diagnosis of extra-CS is suggestive of CS.[104] Characteristic echocardiographic changes suggestive of CS are: wall thickness > 13 mm (due to granulomatous expansion), or < 7 mm (due to fibrosis), aneurysmal dilatation especially at the level of the inferior and posterior walls,[105] regional wall motion abnormalities without any specific coronary distribution, interspersed with normokinetic segments.[106]

CMR is one of the imaging modalities recommended for the diagnosis of CS in current guidelines[103] and CMR may be more sensitive for cardiac involvement than currently used clinical criteria.[107] Myocardial inflammation may be identified by T2 STIR images and early contrast enhancement while areas of fibrosis are detected by LGE[108] (*Figure 12*). The typical pattern of CS on LGE is patchy focal

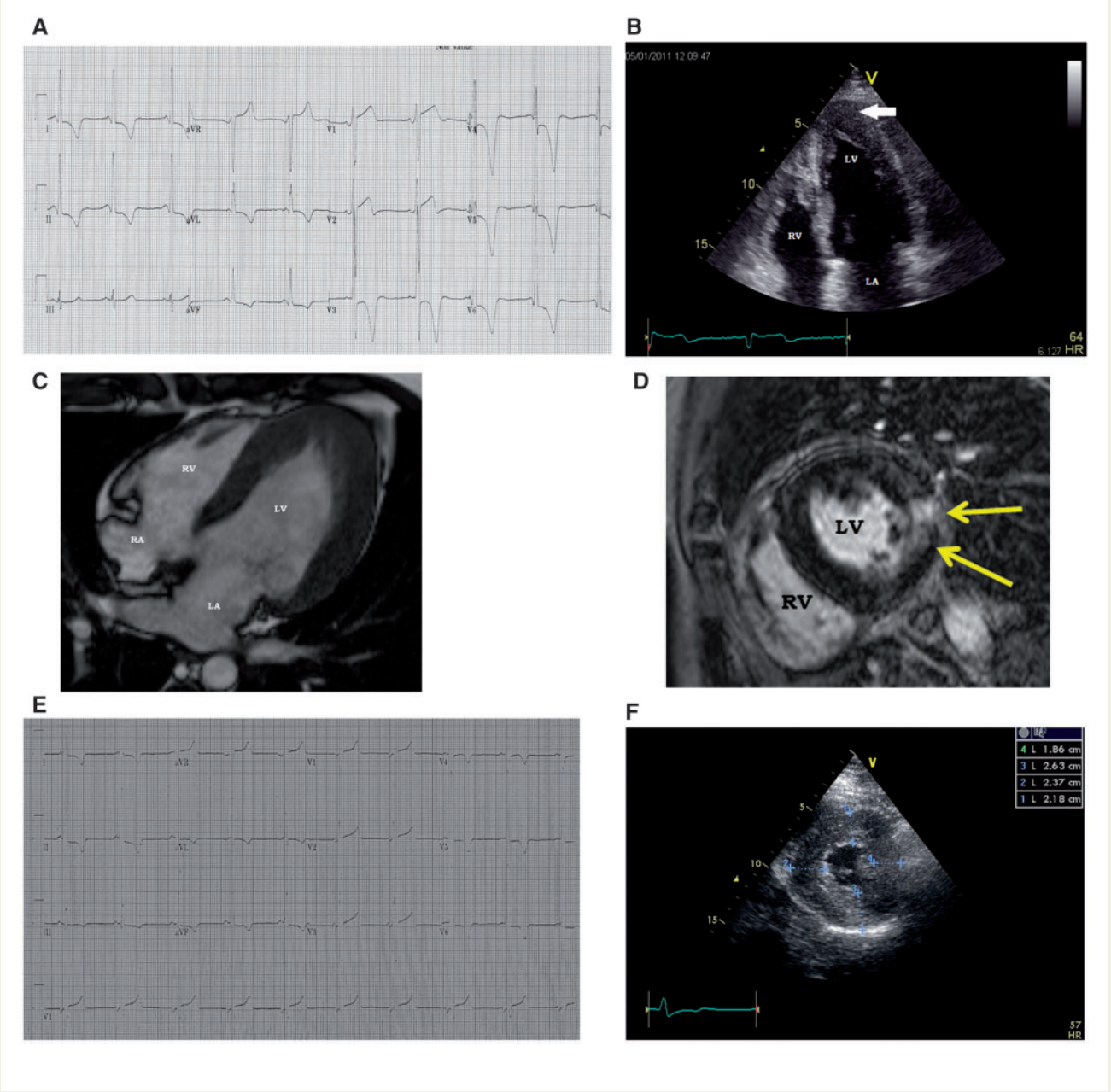

Figure 11 Familial Fabry's disease in two brothers. (*A*) EKG in a 55-year-old male showing a pattern of apical hypertrophy. (*B*) Apical transthoracic view showing an apical hypertrophy (arrow). (*C*) CMR finding of predominantly apical hypertrophy. (*D*) Inferolateral late gadolidium enhancement. (*E*) EKG in his young brother showing milder but similar abnormalities. (*F*) Concentric diffuse hypertrophy in the brother. RV, right ventricle; LV, left ventricle; LA, left atrium; RA, right atrium.

enhancement sparing the endocardial border, not following a coronary artery distribution,[109] and involving mainly the basal and lateral LV walls.[110] Single or often multiple lesions are seen and other, more atypical LGE patterns have also been described. Importantly, no LGE pattern is pathognomonic for CS. Moreover, CMR offers prognostic information: myocardial scar determined by LGE is a predictor for ventricular arrhythmia and sudden cardiac death in patients with sarcoidosis.[111]

Nuclear imaging has also an important role in the assessment of CS. Although the major diagnostic criteria for CS include [67Ga]-citrate scintigraphy, its sensitivity for CS is significantly lower than [18F]FDG-PET/CT.[112] For this reason [18F]FDG-PET/CT have currently replaced [67Ga]-scintigraphy in the majority of centres being nowadays the most commonly used imaging test for detecting myocardial inflammation. Advantages of [18F]FDG-PET/CT over [67Ga] includes favourable tracer kinetics, lower radiation exposure, and better quality images.[113] Active sarcoid lesions present increased [18F]FDG uptake on PET/CT imaging due to utilization of glucose as an energy source by inflammatory cell in infiltrates.[114] However, [18F]FDG-PET/CT has not been officially adopted in the diagnostic

guidelines[115] mainly due to the high variability of [18F]FDG uptake in the normal myocardium, that requires adequate patient preparation to prevent errors. Strategies for myocardial suppression to maximize the accuracy of the procedure include prolonged fasting, dietary modifications, and a heparin load before imaging.[116] The imaging protocol includes preferable gated cardiac [18F]FDG and whole body images.[117] A cardiac perfusion scan could be combined to compare [18F]FDG-PET and perfusion patterns (*Table 4*).[118]

Figure 12 Patient with known CS. The image shows a late gadolinium enhanced CMR image in the vertical long axis plane. Several focal areas of myocardial enhancement can be seen (arrows) consistent with granulomatous myocardial infiltration.

Pitfalls in [18F]FDG PET/CT imaging are myocarditis, CA, infection, and myocardial metastases, causing focal [18F]FDG uptake. There are very few circumstances under which [18F]FDG will be falsely negative as in case of corticosteroids treatment or 'old, non-active' sarcoidosis.

[18F]FDG-PET/CT sensitivity and specificity for CS have been reported at 89% and 78%, respectively.[114] Quantitative analysis further improved these figures, reaching a sensitivity of 97.3% and a specificity of 83.6% for the diagnosis of CS. In addition, standardized uptake value (SUVmax) on [18F]FDG-PET/CT was found the only independent predictor among clinical and imaging variables for diagnosing CS.[119]

Serial [18F]FDG-PET/CT imaging can be utilized to assess the response to therapies. Decrease [18F]FDG uptake in cardiac lesions following therapy has been reported in case of corticosteroid treatment as well as immunosuppressive therapies.[120,121] *Figure 13* illustrates the value of serial [^{18}F]FDG PET/CT in a patient with CS treated with high dose corticosteroids.

[18F]FDG-PET/CT only moderately correlated with CMR, mainly due to the different significance of findings: LGE by CMR represents cardiac damage and scarring whereas [18F]FDG uptake represents active inflammation. When CMR and [18F]FDG -PET/CT were compared with the Japanese Ministry of Health and Welfare guidelines, CMR had a higher specificity with lower sensitivity than nuclear imaging.[122]

In summary, [18F]FDG-PET/CT and CMR are powerful imaging techniques for accurate detection and therapy monitoring of CS. Protocols for imaging with these modalities are increasingly well defined, however large prospective studies supporting new guidelines for CS imaging are warranted.

Systemic sclerosis

Systemic sclerosis (SSc) is a connective tissue disease characterized by vascular and fibrotic lesions of skin and internal organs and represents a model of progressive interstitial myocardial fibrosis triggered

Table 4 Interpretation criteria by combining rest perfusion imaging and FDG findings in suspected cardiac sarcoidosis. Adapted from Blankstein *et al*[118]

Rest perfusion	FDG	Interpretation
Normal perfusion and metabolism		
Normal	No uptake	Negative for CS
Normal	Diffuse	Diffuse FDG most likely due to suboptimal patient preparation
Abnormal perfusion or metabolism		
Normal	Focal	Could represent early disease
Defect[a]	No uptake	Perfusion defect represents scar from sarcoidosis or other aetiology
Abnormal perfusion and metabolism		
Defect	Focal in area of perfusion defect	Active inflammation with scar in the same location
Defect	Focal on diffuse with focal in area of perfusion defect	Active inflammation with scar in the same location with either diffuse inflammation or suboptimal preparation
Defect	Focal in area of normal perfusion	Presence of both scar and inflammation in different segments of the myocardium

CS, cardiac sarcoidosis.
[a]Epicardial coronary artery disease should be always ruled out in these patients, to avoid misinterpretation due to hibernating myocardium.

by increased endothelin production and also focal hypoperfusion.[123] Cardiovascular involvement has been shown to be one of the leading causes of mortality in SSc and can occur in up to 70% of patients as a finding on autopsy.[124,125] Although the primary myocardial involvement remains clinically silent in the majority of patients, it can lead to further diastolic and systolic LV dysfunction,[126] which carries a poor prognosis. Early diagnosis and accurate staging of myocardial involvement are therefore crucial for the management of these patients and for therapeutic strategies.

Conventional echocardiographic assessment of the LVEF has shown limited sensitivity being able to identify only 5% of patients with cardiac involvement.[127] Results of studies using TDI and speckle-tracking echocardiography suggested that myocardial velocity and strain might be more sensitive than conventional measures in identifying subtle cardiac dysfunction in asymptomatic patients with SSc.[128,129]

Since myocardial fibrosis is the primary abnormality underlying SSc cardiac involvement, methods that enable early identification of fibrosis should be preferred. EMB is the gold standard for the detection of myocarditis that may be found in SSc patients and might help to detect cardiac involvement at an early stage of the disease as inflammation was found in 96% and fibrosis in 100% of all SSc patients investigated.[130] Importantly, prognosis was poor and associated with the degree of cardiac inflammation and fibrosis revealing an event rate of 28% within 22.5 months follow-up.[130]

CMR with LGE imaging has been used to detect myocardial areas with replacement fibrosis in patients with an advanced stage of SSc.[131] However, at an early stage of the disease, myocardial fibrosis in SSc is usually diffuse and thus, undetected by LGE-CMR. ECV estimation using pre- and post-contrast T1 mapping has been used to visualize increased collagen content in SSc.[132] A recent study has demonstrated that ECV imaging performed early during SS reveals myocardial abnormalities consistent with diffuse myocardial fibrosis that are not apparent on LGE imaging, therefore representing an early marker of disease.[133] In addition, the ECV abnormalities correlated with diastolic LV dysfunction which occurred in 45% of the patients.[134] This study also evaluated the systolic circumferential strain by CMR that was also found decreased but without any correlation with ECV increase, suggesting therefore that LV systolic dysfunction may be related not only to myocardial fibrosis but also to other phenomena, such as myocardial ischaemia.

In SSc, myocardial ischaemia, unrelated to coronary artery disease, is common with impairment of microcirculation and coronary vasospasm.[135] Therefore, stress echocardiography, CMR stress perfusion and SPECT have been proposed to evaluate myocardial perfusion in SS patients

Non-familial/non-genetic RCM: radiation therapy and cancer drug therapy induced RCM

Cardiac toxicity of radiation therapy

In general, the development of radiotherapy-induced RCM suggests a prior high-dose chest irradiation (>60 Gy). It can also occur at lower

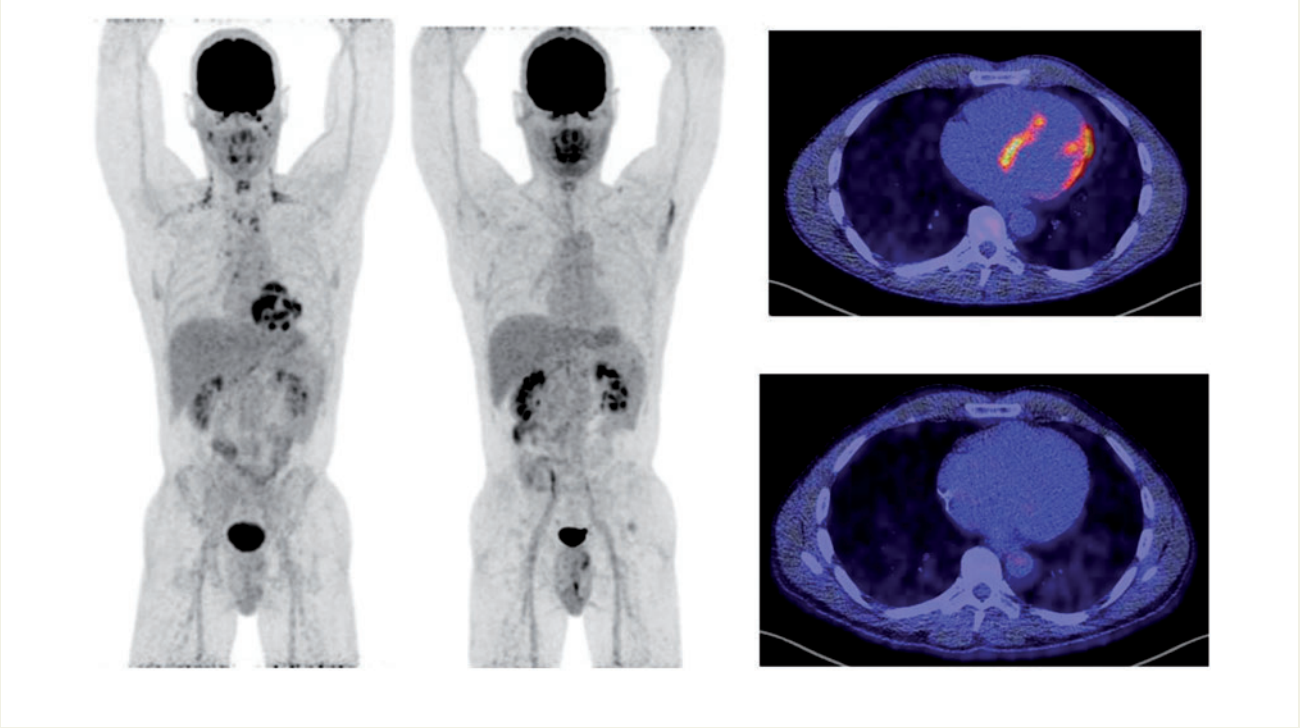

Figure 13 Forty-one year-old male with a total AV block, bradycardia, and weakness. The patient was suspected of CS. Echocardiography was normal. A FDG PET/CT was performed after careful patient preparation with a fatty diet and showed heterogeneous, spotty high uptake in the left ventricle of the heart (left whole body PET and upper row right short axis PET/CT). The patient was treated with high-dose corticosteroids and the repeated FDG PET/CT after 3 months shows fully normalization of the myocardium (right whole body FDG PET/CT and lower short axis PET/CT).

radiation exposure when anthracycline is used.[136] RCM occurs as a result of diffuse myocardial fibrosis. On echocardiography, the classical features of RCM are found. Although its value in radiation-related myocardial fibrosis is still unclear, ECV estimation using pre- and post-contract T1 mapping by CMR is directly related to collagen content.[137] The presence of decreased mean LV mass, end-diastolic dimension, and end-diastolic wall thickness together with dilation of both atria and self-reported dyspnoea, is suggestive of RCM in this population.[138] Cardiac CT has little value in the diagnosis of RCM after radiotherapy, except for the detection of any associated vascular disease. There is no proven value of nuclear cardiology in the detection of RCM after radiation exposure. However, perfusion scintigraphy imaging can reveal fixed regional perfusion defects, which possibly indicate direct damage and the presence of local fibrosis.[139]

Cancer drug induced RCM

The typical structural manifestation of cancer drug induced cardiomyopathy corresponds to a LV eccentric remodelling with dilation of internal cavity and thinning of myocardial walls.[140] When clinical heart failure is overt, this picture is associated with a significant reduction of LV ejection fraction. In the more advanced stages, LV diastolic function can be strongly altered with an abnormal increase of LV filling pressure. This will induce the classic 'restrictive' physiology with the typical standard Doppler-derived transmitral pattern: E/A ratio > 2 or even > 3 and short E velocity deceleration time (usually < 150–160 msec). The presence of a restrictive pattern in a patient with cancer drug induced cardiotoxicity has a recognized prognostic value, exactly as this occurs in the general clinical setting.[8]

Currently, the restrictive diastolic pattern is detectable in particular in patients undergoing anthracyclines (Cardiotoxicity type 1), it being possibly evident not only during treatment (acute cardiotoxicity) but also—and more often—after the completion (even several years after) of cancer therapies.[140] (*Figure 14*, see Supplementary data online, *Videos S6 and S7*). Early cardiotoxicity, occurring during or within 1 year of completion of treatment, is the most important risk factor for the development of late cardiotoxicity, which occurs beyond a year of completion of treatment. This is very important to know in children undergoing anthracyclines therapy. In fact, they can develop late cardiotoxicity during adulthood and should be therefore carefully monitored for years by echocardiography. Cumulative as well as peak anthracycline doses affect adults and children alike.

The restrictive physiology of diastolic pattern is instead very rare in patients undergoing trastuzumab therapy and similar drugs (Cardiotoxicity type 2).[140] This kind of cardiotoxicity is usually reversible with cancer therapy interruption. However, since trastuzumab can be sequentially added to anthracyclines, a combined effect anthracyclines + trastuzumab on the degree of LV filling pressures cannot be excluded and should therefore be carefully monitored.

When a restrictive LV diastolic pattern is detectable in patients receiving cancer drugs, the echocardiographic exam should be extended to a quantitative evaluation of LV longitudinal function. In fact, when high levels of LV filling pressure are evident, a reduction of GLS, measurable by speckle tracking echocardiography, is usually observed. If speckle tracking echocardiography is not available, pulsed tissue Doppler-derived s' velocity of the mitral annulus or even the simple M-mode derived mitral annular plane systolic excursion represent much more than simple surrogates of LV longitudinal dysfunction.

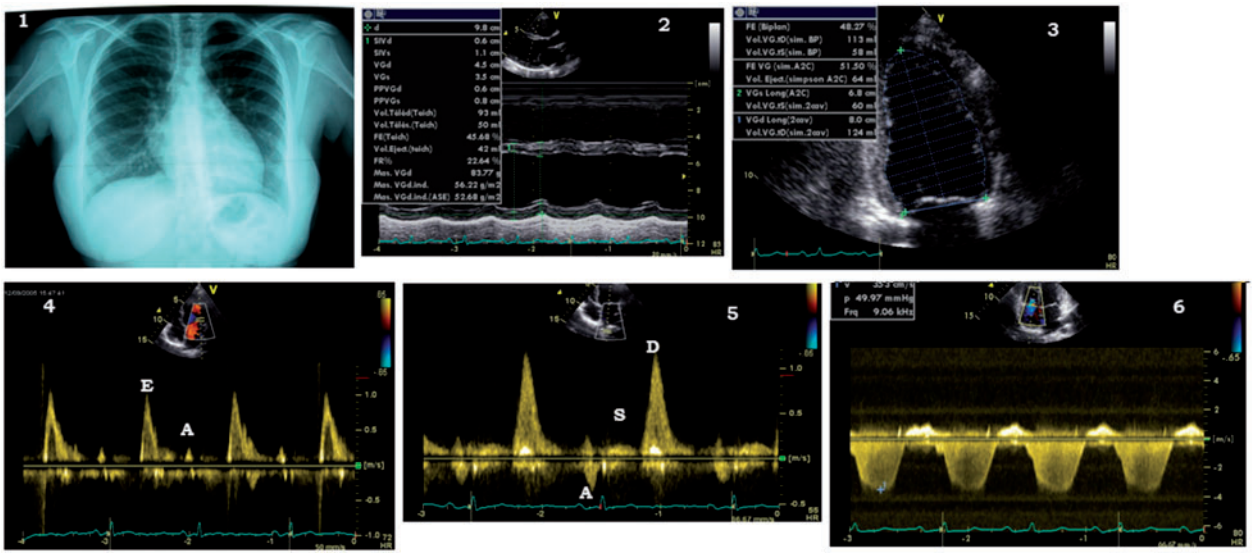

Figure 14 Twenty-five year-old woman treated for Hodgkin disease in infancy with anthracyclins. Chest X ray (1) and echocardiography (2 and 3) show a non-dilated left ventricle, with a relatively preserved LV contractility (Supplementary data online, *Video S6*). However, mitral flow (4) and pulmonary venous flow (5) show a severely restrictive pattern and tricuspid flow recording (6) reveals pulmonary hypertension. Severe longitudinal dysfunction is evidenced by two-dimensional strain (Supplementary data online, *Videos S6 and S7*).

In this cohort of patients, CMR can be useful both for the accurate volumetric assessment with cine imaging but also with the LGE technique for the detection of myocardial fibrosis,[140] i.e. the first determinant of LV diastolic dysfunction and LV filling pressure increase.

Endomyocardial RCMs

Endomyocardial fibrosis

EMF is an often-neglected disorder in the tropical and subtropical regions of the world which is characterized by the development of a RCM,[141] and is associated with a high morbidity and mortality.[142] As etiologic causes of EMF, infections, inflammation, allergy, malnutrition, and toxic agents are discussed.[143] At the histological level, EMF is characterized by a marked endocardial thickening due to the deposition of fibrous tissue (*Figure 15*).[144]

An echocardiographic examination of 1063 individuals revealed that most subjects (55%) had a biventricular involvement, and 28% revealed a right-sided prevalence with mild-moderate structural and functional echocardiographic abnormalities.[145]

Regarding the diagnosis of EMF, transthoracic echocardiographic changes can be useful for visualizing structural abnormalities, especially in chronic EMF.[142,144] The main echocardiographic features include apical obliteration of the left and/or right ventricles, reduced volume of the ventricular cavity, endocardial thickening and a restrictive pattern. (*Figure 16*, see Supplementary data online, *Video S8*)

EMF may be difficult to differentiate from other cardiomyopathies (Loeffler's endocarditis, Churg–Strauss syndrome or rheumatoid arthritis, tuberculous pericarditis, CP, or apical HCM).[142,146–148] After initial echocardiographic analysis, CMR[149] including LGE imaging should be performed which is now the gold standard for imaging the disease. (*Figure 17*) In a CMR study of 36 patients, it was shown that LGE-CMR can provide detailed information on ventricular morphology, including the existence of thrombus or calcifications, and revealing functional information which is useful in the diagnosis and prognosis of EMF through quantification of the typical pattern of the endocardial fibrous tissue deposition.[150] Adjunctive diagnostic tools, such as EMB, can be considered in ambiguous cases[151] and can help in patient management.

Hypereosinophilic syndrome

Eosinophilic EMF is a rare cause of RCM, resulting from toxicity of eosinophils towards cardiac tissues.[152] The causes for eosinophilic infiltration of myocardium are hypersensitivity, parasitic infestation, systemic disease, myeloproliferative syndrome, and idiopathic hypereosinophilic syndrome.[152]

Cardiac disease follows three stages with involvement of the endocardium, the myocardium, and the pericardium. The first is eosinophilic myocarditis (acute necrotic stage) due to infiltration of eosinophils and release of the contents of their granules in the myocardium.[152] There is no relationship between the extent of the infiltrate and clinical symptoms.[153] The intermediate phase is the thrombotic stage, characterized by mural thrombi along the damaged endocardium (more often in the apex of the left ventricle). The third stage is the later fibrotic stage in which the granulation tissue is changed into hyaline fibrosis. The endocardial scar can result in a decrease of ventricular compliance and in RCM.[154]

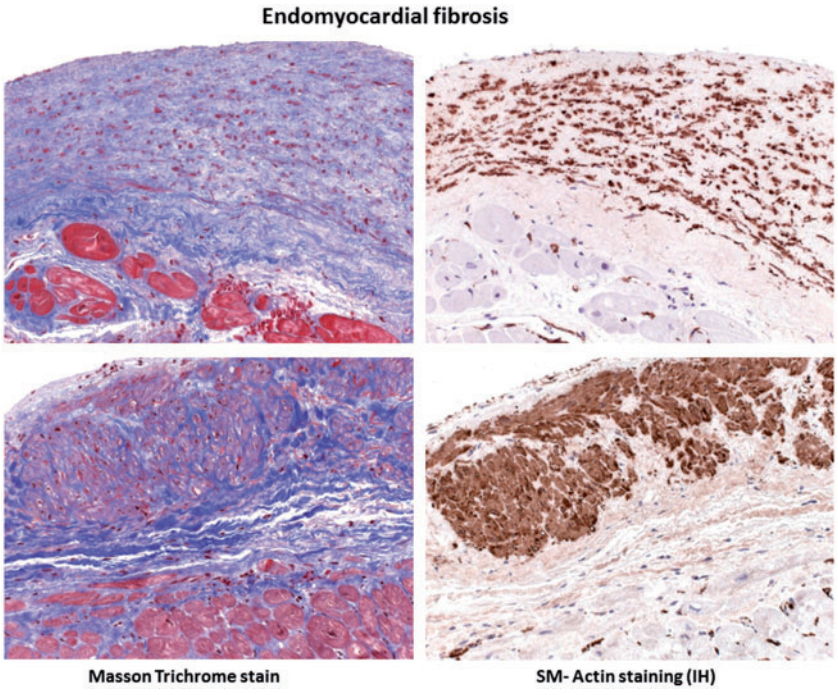

Figure 15 Histologic finding in a patient with EMF.

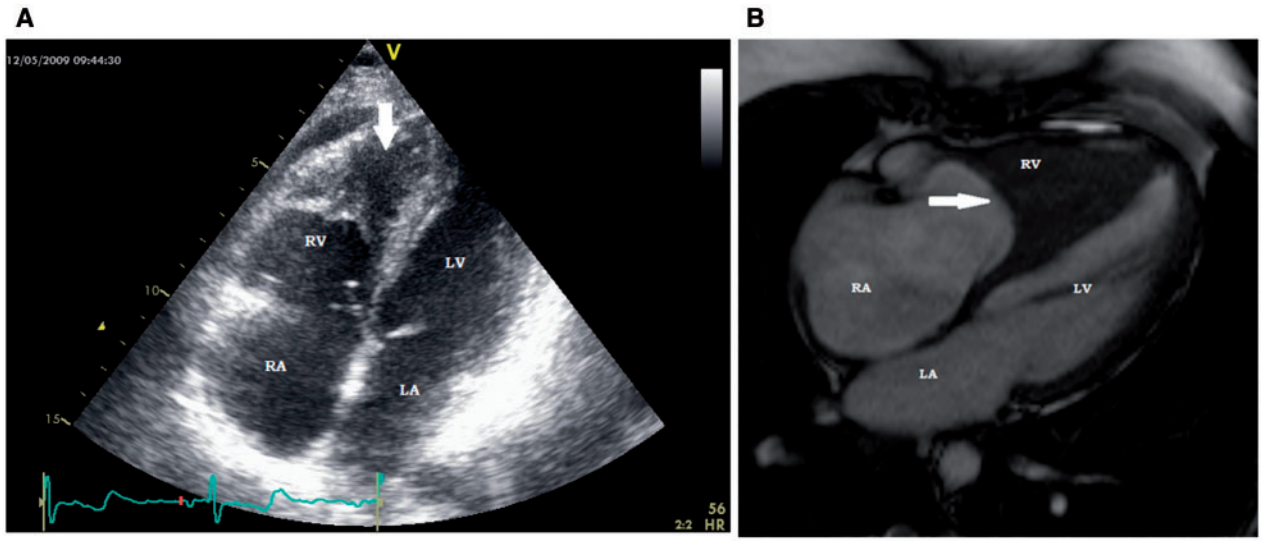

Figure 16 (*A*) (TTE) and (*B*) (CMR) Right ventricular EMF in a 50 year-old woman (Supplementary data online, *Video S8*). The apex of the right ventricle is obliterated (white arrow), with subsequent surgical confirmation. RA, right atrium; RV, right ventricle; LV, left ventricle; LA, left atrium.

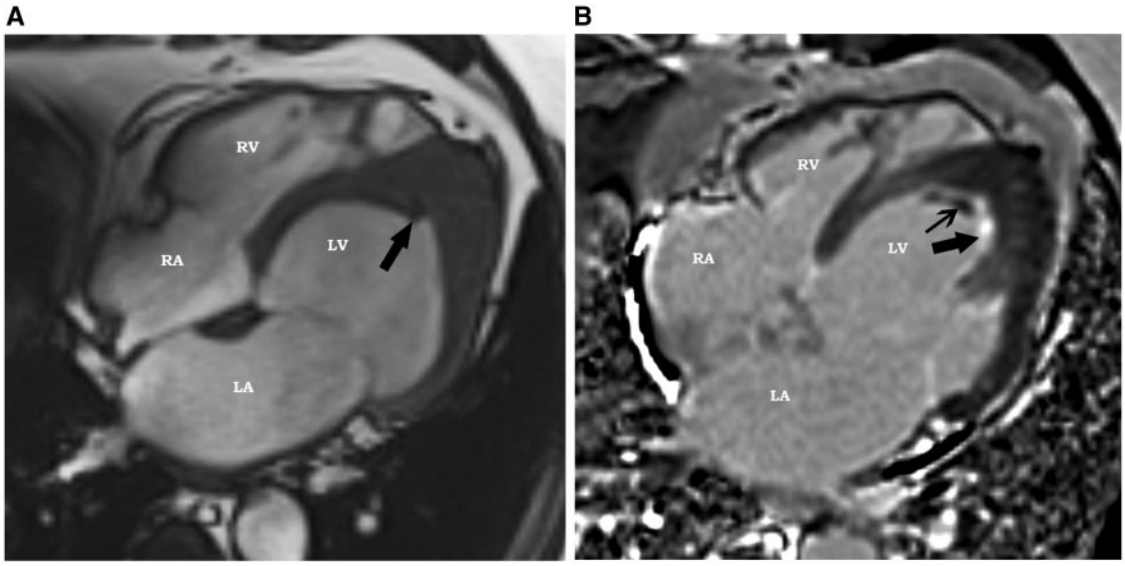

Figure 17 LV EMF in a 58-year-old man presenting with congestive heart failure. (*A*) Cine four chamber view in end-diastolic phase showing a thickening of LV apex (black arrow), a reduced volume of the LV cavity and a left atrial enlargement. (*B*) LGE four chambers view showing a marked endocardial thickening with late gadolinium enhancement (black arrow) and an apical thrombus (open arrow).

On echocardiography, classical findings are progressive endomyocardial thickening, apical obliteration of one or both ventricles by echogenic material suggestive of fibrosis or thrombus formation, posterior mitral leaflet involvement and papillary dysfunction resulting in mitral regurgitation.[154,155] (*Figure 18A*). Pericardial effusion can be present as well as the typical RCM pattern of normal-to-small ventricles with large atria.[156] Echocardiography can also be useful for monitoring the effects of specific therapies on the reversal of endomyocardial infiltration in hypereosinophilic cardiomyopathy.[157]

CMR is very useful in EMF, both for diagnosis of endocardial involvement and for detection of thrombus formation in both

ventricles[158–161] (*Figure 18B*). The gold standard is EMB but the high resolution of CMR and transthoracic echocardiography (TTE) is frequently sufficient for diagnosis and follow-up.[3]

Carcinoid heart disease

Carcinoid heart disease occurs in 20–70% of patients with metastatic carcinoid tumours and will lead to increased morbidity and mortality in these patients.[162] The endocardial fibrosis results in retraction and fixation of the heart valves. Right-sided valves are mainly affected.[163] Left-sided valvular pathology occurs in approximately 10% of patients with carcinoid heart disease and is associated with right-to-left shunting, bronchial carcinoid, or poorly controlled carcinoid syndrome.[164,165]

The hallmarks of carcinoid heart disease are a combination of right-sided valvular dysfunction and typical morphological changes of the valves like valve leaflet thickening, shortening, retraction, reduced mobility, or incomplete coaptation of the tricuspid leaflets.[166–168] CMR has an additive value in carcinoid heart diseases, especially when echocardiography is inconclusive and for accurate measurements of right ventricular function and assessment of carcinoid plaques using LGE.[168] *Figure 19* and Supplementary data online, *Videos S9 and S10* illustrate the value of multimodality imaging in a patient with carcinoid heart disease.

Drug-induced EMF

Animal data suggest the possibility of drug-induced EMF induced by 5-HT2B serotonin receptor agonists such as fenfluramine derivatives, pergolide, cabergolide, and methysergid and ergotamine,[169–171] but very scarce data are currently reported in man. Indeed, only one case of RCM is reported after fenfluramine-phentermine exposure.[172] In addition, a case of sub-aortic obstruction within the LV outflow tract related to drug-induced EMF has been recently reported in a patient exposed to benfluorex, an agonist of 5-HT2B serotoninergic receptors.[173]

Differential diagnosis between RCM and other cardiac diseases

Differential diagnosis between RCM and CP

Differential diagnosis between RCM and CP can be a challenge as their clinical presentation is relatively similar with right heart failure symptoms, preserved LV ejection fraction, and diastolic dysfunction. However, as the treatment of these two conditions is very different, constriction being potentially curable by surgery, making the correct diagnosis is critically important. The differential diagnosis could be performed particularly using the complementary elements obtained from TTE, CMR, cardiac CT, or cardiac catheterization. (*Table 5*)

Cardiac catheterization was the first method historically used to help in the differential diagnosis of RCM and CP, but is not always conclusive.[174,175]

In both RCM and CP, biatrial dilatation, venous dilatation as well as pericardial effusion can be observed. Several echocardiographic parameters have been identified to differentiate myocardial diseases from pericardial constriction.[10,176] In case of RCM, some degree of LV or biventricular hypertrophy or unusual echo texture can be noted (RCM of infiltrative origin). In case of CP, pericardial thickening (>3 mm) or hyperechogenicity of the pericardium can be observed. But one of the main characteristics of CP is the absence of transmission of the intrathoracic pressure variations to the heart, which are physiologically present during the respiratory cycle.

Both TTE and real-time cine CMR allow the identification of some key findings which differentiate the two pathologies: septal bulging occurring with cavity volume variations and the exaggerated respiratory-related LV-RV coupling highlighted by a respiratory septal shift observed in CP and a significant respiratory variation of the diastolic flow. The respiratory septal shift is defined by a difference in the maximal septal excursion into LV between inspiration and expiration (Supplementary data online, *Video S11*).[176] Using CMR, this parameter has a sensitivity of 80% and specificity of 100% to detect CP.[17]

Other echocardiographic findings have been reported to be useful for differentiating RCM and CP, including TDI (e'), E velocity deceleration time, pulmonary vein flow, left atrial volume, and E/e' ratio.[177] *Figure 20* shows an algorithm proposed by the recent ASE/EACVI recommendations for the evaluation of diastolic function by echocardiography,[8] comparing CP and RCM. The presence of a normal annular e' velocity in a patient referred with heart failure diagnosis should raise suspicion of pericardial constriction.[8]

LV myocardial velocities.[178–181] and deformation[11] measured by both TTE and CMR[182] are reduced at a greater degree in RCM compared to CP. Both echocardiography and CMR provide concordant diagnostic information and incremental value for differentiating CP from RCM. Complementary assessment of structural (pericardial thickening), mechanical (myocardial velocities and strains) and haemodynamic (respiratory septal shift) by both TTE and CMR increase the cost-efficacy and confidence for the diagnosis of RCM vs. CP.

Cardiac CT provides excellent anatomic delineation of the pericardium, allowing for accurate measurement of pericardial thickness (abnormal if > 4mm),[183] although a normal pericardial thickness does not exclude CP.[184] Cardiac CT is superior to CMR in detecting pericardial calcifications.[185] Finally, multimodality imaging should be performed in patients with suspected CP, since each imaging modality presents with both advantages and limitations (Table 5, *Figure 21*)

In summary, the differentiation between RCM and CP is frequently difficult and should take into account both clinical presentation and multimodality imaging. The absence of pericardial thickening does not rule out CP. Echocardiography, CMR, and CT provide complementary information and in many patients all three should be performed when CP is suspected.

Differential diagnosis or association between RCM and other myocardial diseases

Although in its most typical « apparently idiopathic » form, RCM presents without LV hypertrophy, in some patients, some forms of cardiomyopathy may resemble or be associated with RCM. Particularly, HCM may resemble RCM in some patients. The classical HCM phenotype presents with enhanced contractility, small cavity, reduced indexed stoke volume, LVOT obstruction, Grade 1 diastolic dysfunction with some fibrosis.[186,187] As the disease progresses,

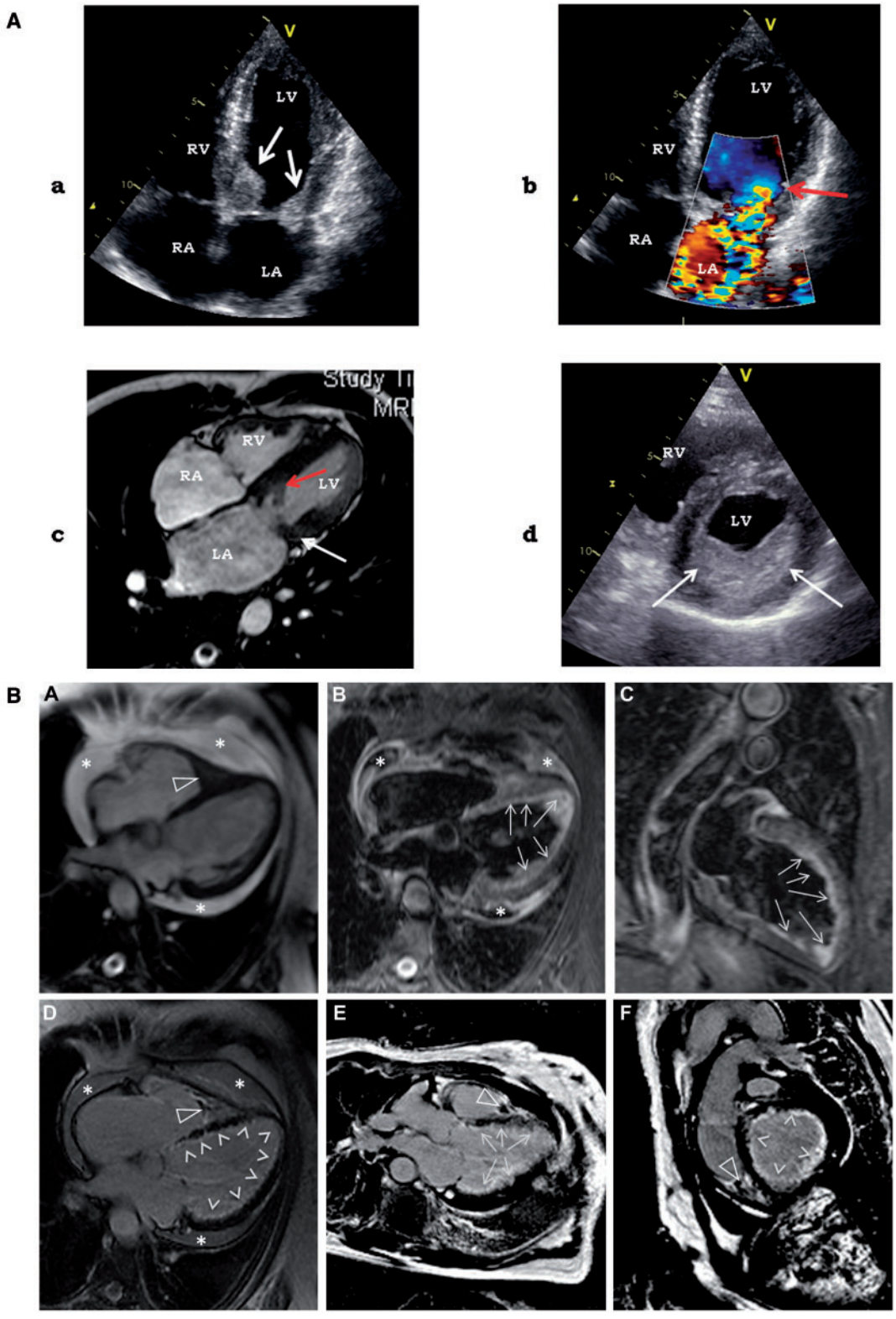

Figure 18 (*A*) Multimodality imaging in hypereosinophilic syndrome with cardiac involvement showing severe restriction of the posterior mitral leaflet associated with involvement of the subvalvular apparatus and severe mitral regurgitation by echocardiography (a, *b*) and CMR (*C*) with worsening in the follow-up (*D*) From reference 155 with permission. RA, right atrium; RV, right ventricle; LV, left ventricle; LA, left atrium. (*B*) CMR in a patient with hypereosinophilic syndrome and Loeffler's syndrome. Cine image (still frame) (*A*) demonstrates a dilated left ventricle and moderate pericardial effusion (asterisks). T2-weighted image (*B* and *C*) shows subendocardial high-signal intensity suggestive of inflammation (white arrows), and T1-weighted images after contrast administration (*D–F*) demonstrate endocardial fibrosis (arrowheads). Of note, an RV apical thrombus is evident in the cine image and in the T1-weighted sequences (triangles) (from [159] with permission).

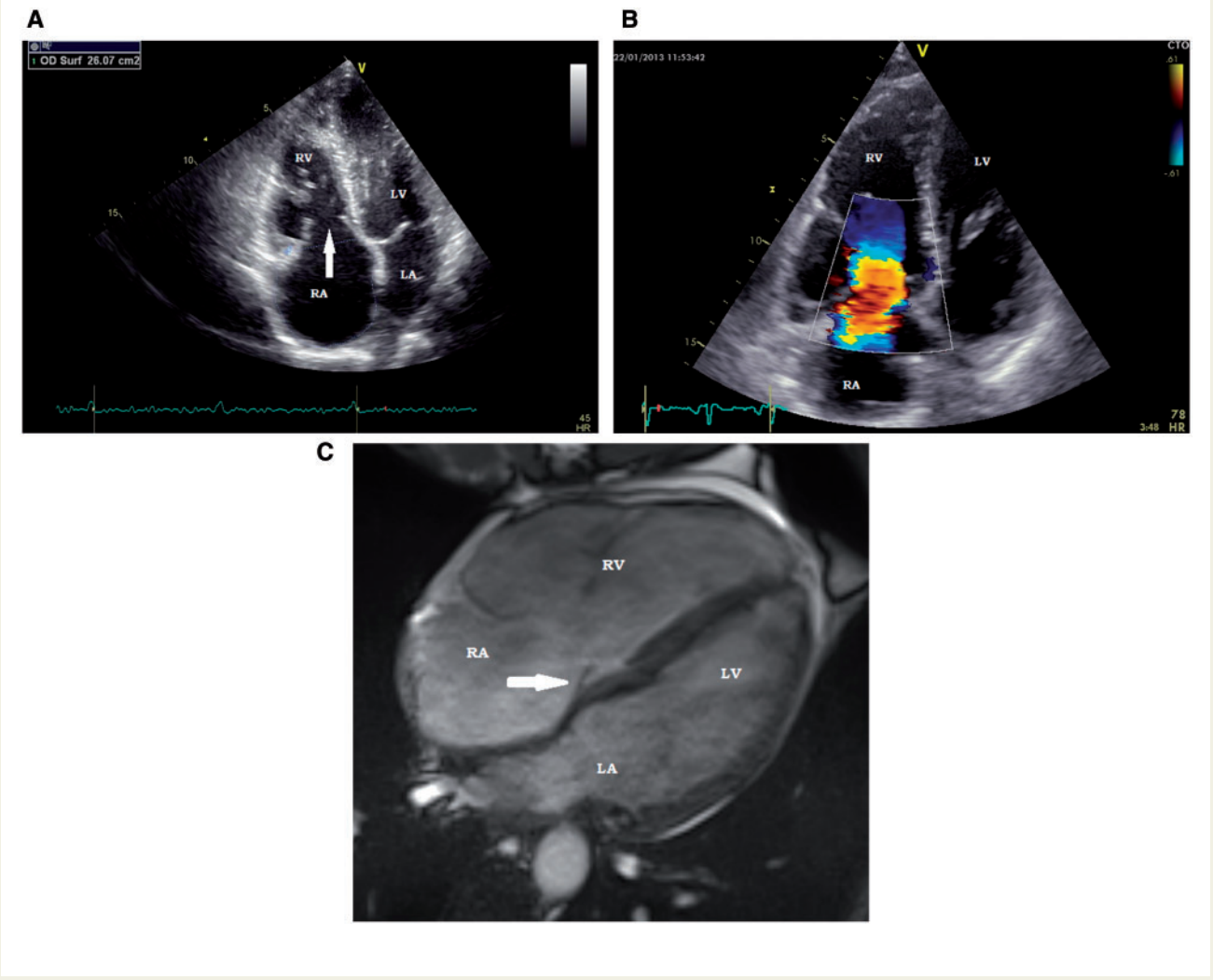

Figure 19 Carcinoid disease with right heart involvement. (*A*) (TTE) and (*C*) (CMR): restriction of the movements of the tricuspid leaflets, which are thickened. The right ventricle myocardium is also involved. (*B*) Massive tricuspid regurgitation (TTE). (*C*) CMR showing dilatation of right heart cavities and restricted tricuspid leaflet (arrow) (Supplementary data online, *Videos S9 and S10*). RA, right atrium; RV, right ventricle; LV, left ventricle; LA, left atrium.

extensive fibrosis,[52] reduced systolic function,[52] diastolic dysfunction,[188,189] marked dilatation of the atria,[190] relative thinning of the LV walls, loss of LVOT obstruction,[190–192] and pulmonary hypertension[192] dominate the picture, mimicking RCM.

Isolated LV non-compaction is a rare form of cardiomyopathy,[193] which should also be differentiated from RCM, but is also sometimes associated with a restrictive pattern or even a true RCM[194] (*Figure 22*, Supplementary data online, *Video S12*)

Conclusion and future directions

RCM represents a heterogeneous group of cardiac diseases with different pathophysiological processes, clinical presentation, treatment, and prognosis. The two main objectives of the clinician are to rule out CP and to find a potentially treatable cause of RCM. Imaging techniques including echocardiography, cardiac CT, CMR, and nuclear techniques are of utmost value for the diagnostic and prognostic assessment of RCM. These techniques give additional information and should frequently be used in combination in the same patient to maximize diagnostic performance. Finally, additional investigations such as EMB, familial screening, and genetic studies are frequently necessary in these patients. For these reasons, patients with suspected RCM should be referred to specialized centres that can provide multimodality imaging and a multidisciplinary team approach.

Supplementary data

Supplementary data are available at *European Heart Journal—Cardiovascular Imaging* online.

Conflict of interest: None declared.

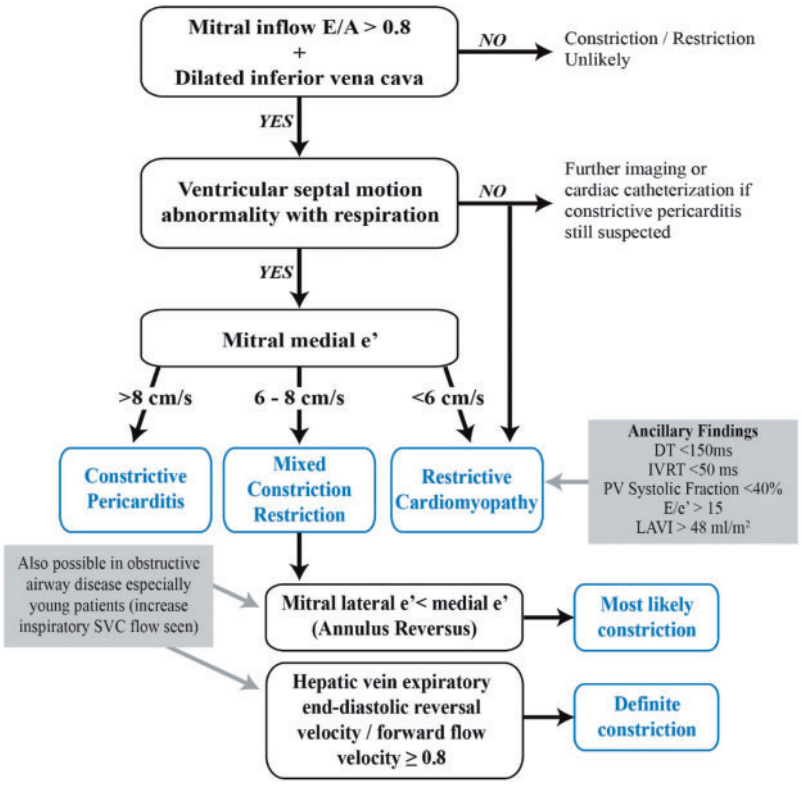

Figure 20 ASE/EACVI algorithm comparing CP and RCM. From [8] with permission.

Table 5 Multimodality imaging to differentiate RCM from constrictive pericarditis

	Constrictive pericarditis	RCM
Chest X-ray		
Pericardial calcification	+++	rare
Two-dimensional and M-mode echocardiography		
Abrupt septal movement ('notch' or 'bounce') in early diastole	+++	0
Septal movement toward left ventricle in inspiration	+++	0
Left atrial enlargement	+	+++
Thick pericardium	+++	0
Pulsed-wave Doppler		
Respiratory variation in mitral and tricuspid flow velocity	>25%	<15%
Diastolic flow reversal in expiration within the hepatic vein	+++	+
TDI		
Mitral medial annulus velocities	e' > 8 cm/s, E/e' < 15	e' < 8 cm/s, E/e' > 15
Deformation imaging		
Reduced longitudinal strain	0	++
Cardiac CT/CMR		
Thick pericardium (cardiac CT)	+++	0
Pericardial calcifications (cardiac CT)	+++	0
Left atrial enlargement (cardiac CT/CMR)	+	+++
Abrupt septal movement ('notch' or 'bounce') in early diastole (CMR)	+++	0
Septal movement toward left ventricle in inspiration (CMR)	+++	0
Reduced longitudinal strain (CMR)	0	++

RCM, restrictive cardiomyopathy; TDI, tissue Doppler imaging; CMR, cardiovascular magnetic resonance; CT, computed tomography.

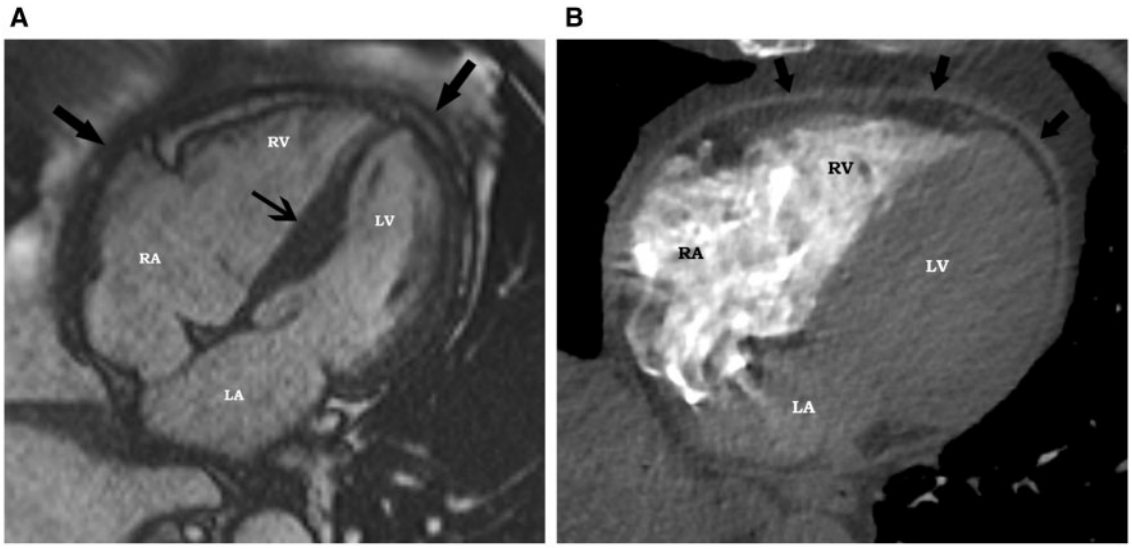

Figure 21 Multimodality imaging in a patient with CP. (*A*) CMR: Cine four chambers view in end-diastolic phase showing a circumferential pericardial thickening (black arrows), biatrial dilatation, and septal convexity inversion (open arrow). (*B*) Cardiac CT: Axial thoracic CT scan showing a circumferential pericardial thickening (black arrows). CMR in CP, illustrating the respiratory septal shift (difference in the maximal septal excursion into LV between inspiration and expiration) (Supplementary data online, *Video S11*).

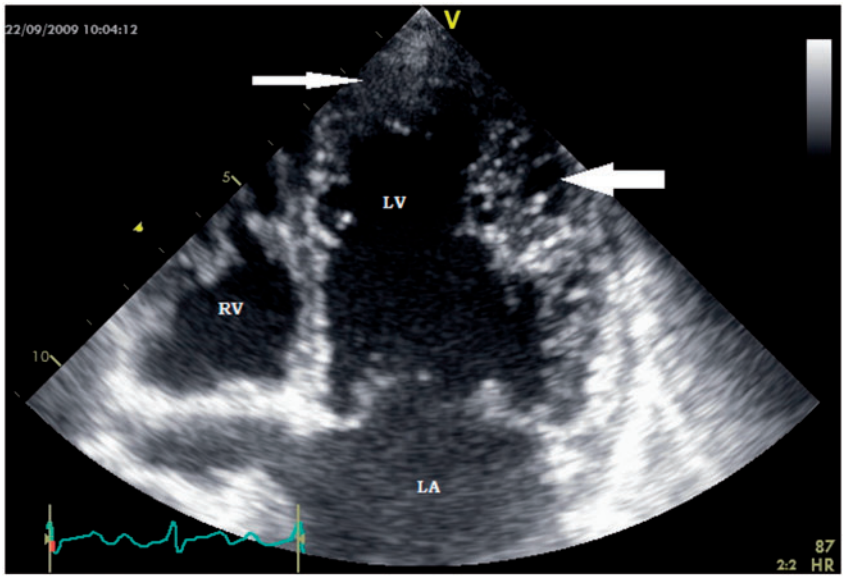

Figure 22 LV hypertrabeculation (arrows) in a young patient with severe RCM (Supplementary data online, *Video S12*).

References

1. Elliott P, Andersson B, Arbustini E, Bilinska Z, Cecchi F, Charron P *et al.* Classification of the cardiomyopathies: a position statement from the European Society Of Cardiology Working Group on Myocardial and Pericardial Diseases. *Eur Heart J* 2008;**29**:270–6.
2. Richardson P, McKenna W, Bristow M, Maisch B, Mautner B, O'Connell J *et al.* Report of the 1995 World Health Organization/International Society and federation of cardiology task force on the definition and classification of cardiomyopathies. *Circulation* 1996;**93**:841–2.
3. Maron BJ, Towbin JA, Thiene G, Antzelevitch C, Corrado D, Arnett D *et al.* Contemporary definitions and classification of the cardiomyopathies: an American Heart Association Scientific Statement from the Council on Clinical

Cardiology, Heart Failure and Transplantation Committee; Quality of Care and Outcomes Research and Functional Genomics and Translational Biology Interdisciplinary Working Groups; and Council on Epidemiology and Prevention. *Circulation* 2006;**113**:1807–16.
4. Nihoyannopoulos P, Dawson D. Restritive cardiomyopathies. *Eur J Echocardiogr* 2009;**10**:23–33.
5. Kushwaha SS, Fallon JT, Fuster V. Restrictive cardiomyopathy. *N Engl J Med* 1997;**336**:267–76.
6. Tam JW, Shaikh N, Sutherland E. Echocardiographic assessment of patients with hypertrophic and restrictive cardiomyopathy: imaging and echocardiography. *Curr Opin Cardiol* 2002;**17**:470–7.
7. Hancock EW. Differential diagnosis of restrictive cardiomyopathy and constrictive pericarditis. *Heart* 2001;**86**:343–9.
8. Nagueh SF, Smiseth OA, Appleton CP, Byrd BF 3rd, Dokainish H, Edvardsen T *et al*. Recommendations for the evaluation of left ventricular diastolic function by echocardiography: an update from the American Society of Echocardiography and the European Association of Cardiovascular Imaging. *Eur Heart J Cardiovasc Imaging* 2016;**17**:1321–60.
9. Klein AL, Hatle LK, Taliercio CP, Oh JK, Kyle RA, Gertz MA *et al*. Prognostic significance of Doppler measures of diastolic function in cardiac amyloidosis. A Doppler echocardiography study. *Circulation* 1991;**83**:808–816.
10. Hyodo E, Hozumi T, Takemoto Y, Watanabe H, Muro T, Yamagishi H *et al*. Early detection of cardiac involvement in patients with sarcoidosis by a non-invasive method with ultrasonic tissue characterisation. *Heart* 2004;**90**:1275–80.
11. Bhandari AK, Nanda NC. Myocardial texture characterization by two-dimensional echocardiography. *Am J Cardiol* 1983;**51**:817
12. Schiano-Lomoriello V, Galderisi M, Mele D, Esposito R, Cerciello G, Buonauro A *et al*. Longitudinal strain of left ventricular basal segments and E/e' ratio differentiate primary cardiac amyloidosis at presentation from hypertensive hypertrophy: an automated function imaging study. *Echocardiography* 2016; doi: 10.1111/echo.13278.
13. Sengupta PP, Krishnamoorthy VK, Abhayaratna WP, Korinek J, Belohlavek M, Sundt TM 3rd *et al*. Disparate patterns of left ventricular mechanics differentiate constrictive pericarditis from restrictive cardiomyopathy. *JACC Cardiovasc Imaging* 2008;**1**:29–38.
14. Kramer CM, Barkhausen J, Flamm SD, Kim RJ, Nagel E. Society for Cardiovascular Magnetic Resonance Board of Trustees Task Force on Standardized Protocols. Standardized cardiovascular magnetic resonance (CMR) protocols 2013 update. *J Cardiovasc Magn Reson* 2013;**15**:91.
15. Bellenger NG, Davies LC, Francis JM, Coats AJ, Pennell DJ. Reduction in sample size for studies of remodeling in heart failure by the use of cardiovascular magnetic resonance. *J Cardiovasc Magn Reson* 2000;**2**:271–8.
16. Cosyns B, Plein S, Nihoyanopoulos P, Smiseth O, Achenbach S, Andrade MJ *et al*; European Association of Cardiovascular Imaging (EACVI); European Society of Cardiology Working Group (ESC WG) on Myocardial and Pericardial diseases. European Association of Cardiovascular Imaging (EACVI) position paper: multimodality imaging in pericardial disease. *Eur Heart J Cardiovasc Imaging* 2015;**16**:12–31.
17. Francone M, Dymarkowski S, Kalantzi M, Rademakers FE, Bogaert J. Assessment of ventricular coupling with real-time cine MRI and its value to differentiate constrictive pericarditis from restrictive cardiomyopathy. *Eur Radiol* 2006;**16**:944–51.
18. Sado DM, White SK, Piechnik SK, Banypersad SM, Treibel T, Captur G *et al*. Identification and assessment of Anderson-Fabry disease by cardiovascular magnetic resonance noncontrast myocardial T1 mapping. *Circ Cardiovasc Imaging* 2013;**6**:392–8.
19. Fontana M, Pica S, Reant P, Abdel-Gadir A, Treibel TA, Banypersad SM *et al*. Prognostic value of late gadolinium enhancement cardiovascular magnetic resonance in cardiac amyloidosis. *Circulation* 2015;**132**:1570–9.
20. Schelbert EB, Piehler KM, Zareba KM, Moon JC, Ugander M, Messroghli DR *et al*. Myocardial fibrosis quantified by extracellular volume is associated with subsequent hospitalization for heart failure, death, or both across the spectrum of ejection fraction and heart failure stage. *J Am Heart Assoc* 2015;**4**:12.
21. Anderson LJ, Holden S, Davis B, Prescott E, Charrier CC, Bunce NH *et al*. Cardiovascular T2-star (T2*) magnetic resonance for the early diagnosis of myocardial iron overload. *Eur Heart J* 2001;**22**:2171–9.
22. Modell B, Khan M, Darlison M, Westwood MA, Ingram D, Pennell DJ. Improved survival of thalassaemia major in the UK and relation to T2* cardiovascular magnetic resonance. *J Cardiovasc Magn Reson* 2008;**10**:42.
23. Karamitsos TD, Piechnik SK, Banypersad SM, Fontana M, Ntusi NB, Ferreira VM *et al*. Noncontrast T1 mapping for the diagnosis of cardiac amyloidosis. *JACC Cardiovasc Imaging* 2013;**6**:488–97.
24. Banypersad SM, Sado DM, Flett AS, Gibbs SD, Pinney JH, Maestrini V *et al*. Quantification of myocardial extracellular volume fraction in systemic AL amyloidosis: an equilibrium contrast cardiovascular magnetic resonance study. *Circ Cardiovasc Imaging* 2013;**6**:34–9.
25. Alam MH, Auger D, McGill LA, Smith GC, He T, Izgi C *et al*. Comparison of 3 T and 1.5 T for T2* magnetic resonance of tissue iron. *J Cardiovasc Magn Reson* 2016;**18**:40.
26. Yared K, Baggish AL, Picard MH, Hoffmann U, Hung J. Multimodality imaging of pericardial diseases. *JACC Cardiovascular imaging* 2010;**3**:650–60.
27. Zhao L, Ma X, Feuchtner GM, Zhang C, Fan Z. Quantification of myocardial delayed enhancement and wall thickness in hypertrophic cardiomyopathy: multidetector computed tomography versus magnetic resonance imaging. *European journal of radiology* 2014;**83**:1778–85.
28. Hamilton-Craig C, Seltmann M, Ropers D, Achenbach S. Myocardial viability by dual-energy delayed enhancement computed tomography. *JACC Cardiovascular imaging* 2011;**4**:207–8.
29. Bandula S, Banypersad SM, Sado D, Flett AS, Punwani S, Taylor SA *et al*. Measurement of tissue interstitial volume in healthy patients and those with amyloidosis with equilibrium contrast-enhanced mr imaging. *Radiology* 2013;**268**:858–64.
30. Kula RW, Engel WK, Line BR. Scanning for soft-tissue amyloid. *Lancet* 1977;**1**:92–3.
31. Aljaroudi WA, Desai MY, Tang WH, Phelan D, Cerqueira MD, Jaber WA. Role of imaging in the diagnosis and management of patients with cardiac amyloidosis: state of the art review and focus on emerging nuclear techniques. *J Nucl Cardiol* 2014;**21**:271–83.
32. Glaudemans AW, van Rheenen RW, van den Berg MP, Noordzij W, Koole M, Blokzijl H *et al*. Bone scintigraphy with (99m)technetium-hydroxymethylene diphosphonate allows early diagnosis of cardiac involvement in patients with transthyretin-derived systemic amyloidosis. *Amyloid* 2014;**21**:35–44.
33. Minutoli F, Di Bella G, Mazzeo A, Donato R, Russo M, Scribano E *et al*. Comparison between (99m)Tc-diphosphonate imaging and MRI with late gadolinium enhancement in evaluating cardiac involvement in patients with transthyretin familial amyloid polyneuropathy. *AJR Am J Roentgenol* 2013;**200**:W256–65.
34. Coutinho MC, Cortez-Dias N, Cantinho G, Conceição I, Oliveira A, Bordalo e Sá A *et al*. Reduced myocardial 123-iodine metaiodobenzylguanidine uptake: a prognostic marker in familial amyloid polyneuropathy. *Circ Cardiovasc Imaging* 2013;**6**:627–36.
35. Youssef G, Beanlands RSB, Birnie DH, Nery PB. Cardiac sarcoidosis: applications of imaging in diagnosis and directing treatment. *Heart* 2011;**97**:2078–87.
36. Ohira H, Tsujino I, Ishimaru S, Oyama N, Takei T, Tsukamoto E *et al*. Myocardial imaging with 18F-fluoro-2-deoxyglucose positron emission tomography and magnetic resonance imaging in sarcoidosis. *Eur J Nucl Med Mol Imaging* 2008;**35**:933–41.
37. Apgral R, Dweck MR, Trivieri MG, Robson PM, Karakatsanis N, Mani V *et al*. Clinical Utility of Combined FDG-PET/MR to Assess Myocardial Disease. *JACC Cardiovasc Imaging 2016 Jun 29*; pii:S1936-878X(16)30259–5. doi: 10.1016/j.jcmg.2016.02.029 [Epub ahead of print].
38. Mogensen J, Arbustini E. Restrictive cardiomyopathy. *Curr Opin Cardiol* 2009;**24**:214–20.
39. Arbustini E, Morbini P, Grasso M, Fasani R, Verga L, Bellini O *et al*. Restrictive cardiomyopathy, atrioventricular block and mild to subclinical myopathy in patients with desmin-immunoreactive material deposits. *J Am Coll Cardiol* 1998;**31**:645–53.
40. Arbustini E, Buonanno C, Trevi G, Pennelli N, Ferrans VJ, Thiene G. Cardiac ultrastructure in primary restrictive cardiomyopathy. *Chest* 1983;**84**:236–8.
41. Cannavale A, Ordovas KG, Rame EJ, Higgins CB. Hypertrophic cardiomyopathy with restrictive phenotype and myocardial crypts. *J Thorac Imaging* 2010;**25**:W121–3.
42. Rapezzi C, Lorenzini M, Longhi S, Milandri A, Gagliardi C, Bartolomei I *et al*. Cardiac amyloidosis: the great pretender. *Heart Fail Rev* 2015;**20**:117–24.
43. Rapezzi C, Arbustini E, Caforio AL *et al*. Diagnostic work-up in cardiomyopathies: bridging the gap between clinical phenotypes and final diagnosis. A position statement from the ESC Working Group on Myocardial and Pericardial Diseases. *Eur Heart J* 2013;**34**:1448–58.
44. Koyama J, Ikeda S, Ikeda U. Echocardiographic assessment of the cardiac amyloidoses. *Circ J* 2015;**79**:721–34.
45. Feng D, Edwards WD, Oh JK, Chandrasekaran K, Grogan M, Martinez MW *et al*. Intracardiac thrombosis and embolism in patients with cardiac amyloidosis. *Circulation* 2007;**116**:2420–6.
46. Innelli P, Galderisi M, Catalano L, Martorelli MC, Olibet M, Pardo M *et al*. Detection of increased left ventricular filling pressure by pulsed tissue Doppler in cardiac amyloidosis. *J Cardiovasc Med* 2006;**7**:742–7.
47. Tendler A, Helmke S, Teruya S, Alvarez J, Maurer MS. The myocardial contraction fraction is superior to ejection fraction in predicting survival in patients with AL cardiac amyloidosis. *Amyloid* 2015;**22**:61–6.
48. Phelan D, Collier P, Thavendiranathan P, Popović ZB, Hanna M, Plana JC *et al*. Relative apical sparing of longitudinal strain using two-dimensional speckle-tracking echocardiography is both sensitive and specific for the diagnosis of cardiac amyloidosis. *Heart* 2012;**98**:1442–8.

49. Schiano-Lomoriello V, Galderisi M, Mele D, Esposito R, Cerciello G, Buonauro A *et al.* Longitudinal strain of left ventricular basal segments and E/e' ratio differentiate primary cardiac amyloidosis at presentation from hypertensive hypertrophy: an automated function imaging study. *Echocardiography* 2016;**33**:1335–43.
50. Bellavia D, Pellikka PA, Al-Zahrani GB, Abraham TP, Dispenzieri A, Miyazaki C *et al.* Independent predictors of survival in primary systemic (Al) amyloidosis, including cardiac biomarkers and left ventricular strain imaging: an observational cohort study. *J Am Soc Echocardiogr* 2010;**23**:643–52.
51. Ternacle J, Bodez D, Guellich A, Audureau E, Rappeneau S, Lim P *et al.* Causes and consequences of longitudinal LV dysfunction assessed by 2D strain echocardiography in cardiac amyloidosis. *JACC Cardiovasc Imaging* 2016;**9**:126–38.
52. Quarta CC, Solomon SD, Uraizee I, Kruger J, Longhi S, Ferlito M *et al.* Left Ventricular structure and function in TTR-related versus AL cardiac amyloidosis. *Circulation* 2014;**129**:1840–9.
53. Maceira AM, Joshi J, Prasad SK, Moon JC, Perugini E, Harding I *et al.* Cardiovascular magnetic resonance in cardiac amyloidosis. *Circulation* 2005;**111**:186–93.
54. Vogelsberg H, Mahrholdt H, Deluigi CC, Yilmaz A, Kispert EM, Greulich S *et al.* Cardiovascular magnetic resonance in clinically suspected cardiac amyloidosis: noninvasive imaging compared to endomyocardial biopsy. *J Am Coll Cardiol* 2008;**51**:1022–30.
55. Syed IS, Glockner JF, Feng D, Araoz PA, Martinez MW, Edwards WD *et al.* Role of cardiac magnetic resonance imaging in the detection of cardiac amyloidosis. *JACC Cardiovasc Imaging* 2010;**3**:155–64.
56. Fontana M, Banypersad SM, Treibel TA, Abdel-Gadir A, Maestrini V, Lane T *et al.* Differential myocyte responses in patients with cardiac transthyretin amyloidosis and light-chain amyloidosis: a cardiac MR imaging study. *Radiology* 2015;**277**:388–97.
57. Di Bella G, Pizzino F, Minutoli F, Zito C, Donato R, Dattilo G *et al.* The mosaic of the cardiac amyloidosis diagnosis: role of imaging in subtypes and stages of the disease. *Eur Heart J Cardiovasc Imaging* 2014;**15**:1307–15.
58. Bokhari S, Castano A, Pozniakoff T, Deslisle S, Latif F, Maurer MS. (99m)Tc-pyrophosphate scintigraphy for differentiating light-chain cardiac amyloidosis from the transthyretin-related familial and senile cardiac amyloidoses. *Circ Cardiovasc Imaging* 2013;**6**:195–201.
59. Hutt DF, Quigley AM, Page J, Hall ML, Burniston M, Gopaul D *et al.* Utility and limitations of 3,3-diphosphono-1,2-propanodicarboxylic acid scintigraphy in systemic amyloidosis. *Eur Heart J Cardiovasc Imaging* 2014;**15**:1289–98.
60. Perugini E, Guidalotti PL, Salvi F, Cooke RM, Pettinato C, Riva L *et al.* Noninvasive etiologic diagnosis of cardiac amyloidosis using 99mTc-3,3-diphosphono-1,2-propanodicarboxylic acid scintigraphy. *J Am Coll Cardiol* 2005;**46**:1076–84.
61. Rapezzi C, Quarta CC, Guidalotti PL, Pettinato C, Fanti S, Leone O *et al.* Role of (99m)Tc-DPD scintigraphy in diagnosis and prognosis of hereditary transthyretin-related cardiac amyloidosis. *JACC Cardiovasc Imaging* 2011;**4**:659–70.
62. Gillmore JD, Maurer MS, Falk RH, Merlini G, Damy T, Dispenzieri A *et al.* Nonbiopsy diagnosis of cardiac transthyretin amyloidosis. *Circulation* 2016;**133**:2404–12.
63. Cardim N, Galderisi M, Edvardsen T, Plein S, Popescu BA, D'Andrea A *et al.* Role of multimodality cardiac imaging in the management of patients with hypertrophic cardiomyopathy: an expert consensus of the European Association of Cardiovascular Imaging Endorsed by the Saudi Heart Association. *Eur Heart J Cardiovasc Imaging* 2015;**16**:280.
64. Bosi G, Crepaz R, Gamberini MR, Fortini M, Scarcia S, Bonsante E *et al.* Left ventricular remodelling, and systolic and diastolic function in young adults with beta thalassaemia major: a Doppler echocardiographic assessment and correlation with haematological data. *Heart* 2003;**89**:762–6.
65. Leon MB, Borer JS, Bacharach SL, Green MV, Benz EJ Jr, Griffith P *et al.* Detection of early cardiac dysfunction in patients with severe beta-thalassemia and chronic iron overload. *N Engl J Med* 1979;**301**:1143–8.
66. Kremastinos DT, Farmakis D, Aessopos A, Hahalis G, Hamodraka E, Tsiapras D *et al.* Beta-thalassemia cardiomyopathy: history, present considerations, and future perspectives. *Circ Heart Fail* 2010;**3**:451–8.
67. Cogliandro T, Derchi G, Mancuso L, Mayer MC, Pannone B, Pepe A *et al.* Society for the Study of Thalassemia and Hemoglobinopathies (SoSTE). Guideline recommendations for heart complications in thalassemia major. *J Cardiovasc Med* 2008;**9**:515–25.
68. Efthimiadis GK, Hassapopoulou HP, Tsikaderis DD, Karvounis HI, Giannakoulas GA, Parharidis GE *et al.* Survival in thalassaemia major patients. *Circ J* 2006;**70**:1037–42.
69. Giakoumis A, Berdoukas V, Gotsis E, Aessopos A. Comparison of echocardiographic (US) volumetry with cardiac magnetic resonance imaging in transfusion dependent thalassemia major. *Cardiovasc Ultrasound* 2007;**5**:24.
70. Pennell DJ, Udelson JE, Arai AE, Bozkurt B, Cohen AR, Galanello R *et al.* American Heart Association Committee on Heart Failure and Transplantation of the Council on Clinical Cardiology and Council on Cardiovascular Radiology and Imaging. Cardiovascular function and treatment in β-thalassemia major: a consensus statement from the American Heart Association. *Circulation* 2013;**128**:281–308.
71. Pepe A, Meloni A, Capra M, Cianciulli P, Prossomariti L, Malaventura C *et al.* Deferasirox, deferiprone and desferrioxamine treatment in thalassemia major patients: cardiac iron and function comparison determined by quantitative magnetic resonance imaging. *Haematologica* 2011;**96**:41–7.
72. Meloni A, Positano V, Ruffo GB, Spasiano A, D'Ascola D, Peluso A *et al.* Improvement of heart iron with preserved patterns of iron store by CMR-guided chelation therapy. *European Heart J Cardiovasc Imaging* 2015;**16**:325–34.
73. Casale M, Meloni A, Filosa A, Cuccia L, Caruso V, Palazzi G *et al.* Multiparametric cardiac magnetic resonance survey in children with thalassemia major a multicenter study. *Circ Cardiovasc Imaging* 2015;**8**:e003230.
74. Pepe A, Positano V, Capra M, Maggio A, Pinto CL, Spasiano A *et al.* Myocardial scarring by delayed enhancement cardiovascular magnetic resonance in thalassaemia major. *Heart* 2009;**95**:1688–93.
75. Linhart A, Kampmann C, Zamorano JL, Sunder-Plassmann G, Beck M, Mehta A *et al.* European FOS Investigators. Cardiac manifestations of Anderson-Fabry disease: results from the international Fabry outcome survey. *Eur Heart J* 2007;**28**:1228–35.
76. MacDermot KD, Holmes A, Miners AH. Natural history of Fabry disease in affected males and obligate carrier females. *J Inherit Metab Dis* 2001;**24**(Suppl 2):13–4.
77. Gambarin FI, Disabella E, Narula J, Diegoli M, Grasso M, Serio A *et al.* When should cardiologists suspect Anderson-Fabry disease? *Am J Cardiol* 2010;**106**:1492–9.
78. West M, Nicholls K, Mehta A, Clarke JT, Steiner R, Beck M *et al.* Agalsidase alpha and kidney dysfunction in Fabry disease. *J Am Soc Nephrol* 2009;**20**:1132–9.
79. Perrot A, Osterziel KJ, Beck M, Dietz R, Kampmann C. Fabry disease: focus on cardiac manifestations and molecular mechanisms. *Herz* 2002;**27**:699–702.
80. Nagueh SF. Anderson-Fabry disease and other lysosomal storage disorders. *Circulation* 2014;**130**:1081–90.
81. Weidemann F, Linhart A, Monserrat L, Strotmann J. Cardiac challenges in patients with Fabry disease. *Int J Cardiol* 2010;**141**:3–10.
82. Hoigné P, Attenhofer Jost CH, Duru F, Oechslin EN, Seifert B, Widmer U *et al.* Simple criteria for differentiation of Fabry disease from amyloid heart disease and other causes of left ventricular hypertrophy. *Int J Cardiol* 2006;**111**:413–22.
83. Feriozzi S, Schwarting A, Sunder-Plassmann G, West M, Cybulla M. International Fabry Outcome Survey Investigators. Agalsidase alpha slows the decline in renal function in patients with Fabry disease. *Am J Nephrol* 2009;**29**:353–61.
84. Pieroni M, Chimenti C, Russo A, Russo MA, Maseri A, Frustaci A. Tissue Doppler imaging in Fabry disease. *Curr Opin Cardiol* 2004;**19**:452–7.
85. Toro R, Perez-Isla L, Doxastaquis G, Barba MA, Gallego AR, Pintos G *et al.* Clinical usefulness of tissue Doppler imaging in predicting preclinical Fabry cardiomyopathy. *Int J Cardiol* 2009;**132**:38–44.
86. Zamorano J, Serra V, Pérez de Isla L, Feltes G, Calli A, Barbado FJ *et al.* Usefulness of tissue Doppler on early detection of cardiac disease in Fabry patients and potential role of enzyme replacement therapy (ERT) for avoiding progression of disease. *Eur J Echocardiogr* 2011;**12**:671–7.
87. De Cobelli F, Esposito A, Belloni E, Pieroni M, Perseghin G, Chimenti C *et al.* Delayed-enhanced cardiac MRI for differentiation of Fabry's disease from symmetric hypertrophic cardiomyopathy. *AJR Am J Roentgenol* 2009;**192**: W97-102.
88. Boucek D, Jirikowic J, Taylor M. Natural history of Danon disease. *Genet Med* 2011;**13**:563–8.
89. Maron BJ, Roberts WC, Arad M, Haas TS, Spirito P, Wright GB *et al.* Clinical outcome and phenotypic expression in LAMP2 cardiomyopathy. *JAMA* 2009;**301**:1253–9.
90. D'souza RS, Levandowski C, Slavov D, Graw SL, Allen LA, Adler E *et al.* Danon disease: clinical features, evaluation, and management. *Circ Heart Fail* 2014;**7**:843–9.
91. Gussenhoven WJ, Busch HF, Kleijer WJ, de Villeneuve VH. Echocardiographic features in the cardiac type of glycogen storage disease II. *Eur Heart J* 1983;**4**:41–3.
92. Rees A, Elbl F, Minhas K, Solinger R. Echocardiographic evidence of outflow tract obstruction in Pompe's disease (glycogen storage disease of the heart). *Am J Cardiol* 1976;**37**:1103–6.
93. Barker PC, Pasquali SK, Darty S, Ing RJ, Li JS, Kim RJ *et al.* Use of cardiac magnetic resonance imaging to evaluate cardiac structure, function and fibrosis in children with infantile Pompe disease on enzyme replacement therapy. *Mol Genet Metab* 2010;**101**:332–7.
94. Nucifora G, Miani D, Piccoli G, Proclemer A. Cardiac magnetic resonance imaging in Danon disease. *Cardiology* 2012;**121**:27–30.
95. Wei LG, Gao JQ, Liu XM, Huang JM, Li XZ. A study of glycogen storage disease with 99Tcm-MIBI gated myocardial perfusion imaging. *Ir J Med Sci* 2013;**182**:615–20.

96. Lo Iudice F, Barbato A, Muscariello R, Di Nardo C, de Stefano F, Sibilio M *et al* . Left ventricular diastolic dysfunction in type I Gaucher Disease: An Echo Doppler Study. *Echocardiography* 2015;**32**:890–5.
97. Braunlin E, Wang R. Cardiac issues in adults with mucopolysaccharidoses; current knowledge and emerging needs. *Heart* 2016;**102**:1257–62.
98. Przybojewski JZ, Maritz F, Tiedt FA, van der Walt JJ. Pseudoxanthoma elasticum with cardiac involvement. A case report and review of the literature. *S Afr Med J* 1981;**59**:268–75.
99. Campens L, Vanakker OM, Trachet B, Segers P, Leroy BP, De Zaeytijd J *et al*. Characterization of cardiovascular involvement in pseudoxanthoma elasticum families. *Arterioscler Thromb Vasc Biol* 2013;**33**:2646–52.
100. Nguyen LD, Terbah M, Daudon P, Martin L. Left ventricular systolic and diastolic function by echocardiogram in pseudoxanthoma elasticum. *Am J Cardiol* 2006;**97**:1535–7.
101. Sabán-Ruiz J, Fabregate Fuente R, Sánchez-Largo Uceda E, Fabregate Fuente M. Pseudoxanthoma elasticum: case report with arterial stiffness evaluated by a research cardiovascular profiling system. *Eur J Dermatol* 2010;**20**:785–7.
102. Kandolin R, Lehtonen J, Airaksinen J, Vihinen T, Miettinen H, Ylitalo K *et al*. Cardiac sarcoidosis: epidemiology, characteristics, and outcome over 25 years in a nationwide study. *Circulation* 2015;**131**:624–32.
103. Birnie DH, Sauer WH, Bogun F, Cooper JM, Culver DA, Duvernoy CS *et al*. HRS expert consensus statement on the diagnosis and management of arrhythmias associated with cardiac sarcoidosis. *Heart Rhythm* 2014;**11**:1305–23.
104. Judson MA, Costabel U, Drent M, Wells A, Maier L, Koth L *et al*. Organ Assessment Instrument Investigators TW. The WASOG Sarcoidosis Organ Assessment Instrument: An update of a previous clinical tool. *Sarcoidosis Vasc Diffuse Lung Dis* 2014;**31**:19–27.
105. Chiu CZ, Nakatani S, Yamagishi M, Miyatake K, Cheng JJ. Echocardiographic Manifestations in Patients with Cardiac Sarcoidosis, *J Med Ultrasound* 2002;**10**:135–40.
106. Hourigan LA, Burstow DJ, Pohlner P, Clarke BE, Donnelly JE. Transesophageal echocardiographic abnormalities in a case of cardiac sarcoidosis. *J Am Soc Echocardiogr* 2001;**14**:399–402.
107. Patel MR, Cawley PJ, Heitner JF, Klem I, Parker MA, Jaroudi WA. Detection of myocardial damage in patients with sarcoidosis. *Circulation* 2009;**120**:1969–77.
108. Hundley WG, Bluemke DA, Finn JP, Flamm SD, Fogel MA, Friedrich MG *et al*. ACCF/ACR/AHA/NASCI/SCMR 2010 expert consensus document on cardiovascular magnetic resonance: a report of the American College of Cardiology Foundation Task Force on Expert Consensus Documents. *J Am Coll Cardiol* 2010;**55**:2614–62.
109. Schulz-Menger J, Wassmuth R, Abdel-Aty H, Siegel I, Franke A, Dietz R, Friedrich M G. Patterns of myocardial inflammation and scarring in sarcoidosis as assessed by cardiovascular magnetic resonance. *Heart* 2006;**92**:399–400.
110. Seward JB, Casaclang-Verzosa G. Infiltrative cardiovascular diseases: cardiomyopathies that look alike. *J Am Coll Cardiol* 2010;**55**:1769–79.
111. Lancefield T, Voskoboinik A, Taylor AJ, Nadel J. Late gadolinium enhancement identified with cardiac magnetic resonance imaging in sarcoidosis patients is associated with long-term ventricular arrhythmia and sudden cardiac death. *Eur Heart J Cardiovasc Imaging* 2015;**16**:634–41.
112. Okumura W, Iwasaki T, Toyama T, Iso T, Arai M, Oriuchi N *et al*. Usefulness of fasting 18F-FDG PET in identification of cardiac sarcoidosis. *J Nucl Med* 2004;**45**:1989–98.
113. Keijsers RG, Grutters JC, Thomeer M, Du Bois RM, Van Buul MM, Lavalaye FJ. *et al*. Imaging the inflammatory activity of sarcoidosis: sensitivity and inter observer agreement of (67)Ga imaging and (18)F-FDG PET. *Q J Nucl Med Mol Imaging* 2011;**55**:66–71
114. Ishimaru S, Tsujino I, Takei T, Tsukamoto E, Sakaue S, Kamigaki M *et al*. Focal uptake on 18F-fluoro-2-deoxyglucose positron emission tomography images indicates cardiac involvement of sarcoidosis. *Eur Heart J* 2005;**26**:1538–43.
115. Youssef G, Leung E, Mylonas I, Nery P, Williams K, Wisenberg G *et al*. The use of 18F-FDG PET in the diagnosis of cardiac sarcoidosis: a systematic review and metaanalysis including the Ontario experience. *J Nucl Med* 2012;**53**:241–8.
116. Tang R, Wang JT, Wang L, Le K, Huang Y, Hickey AJ *et al*. Impact of patient preparation on the diagnostic performance of 18F-FDG PET in cardiac sarcoidosis: a systematic review and meta-analysis. *Clin Nucl Med* 2016;**41**:e327-39.
117. Skali H, Schulman AR, Dorbala S. (18)F-FDG PET/CT for the assessment of myocardial sarcoidosis. *Curr Cardiol Rep* 2013;**15**:352.
118. Blankstein R, Osborne M, Naya M, Waller A, Kim CK, Murthy VL *et al*. Cardiac positron emission tomography enhances prognostic assessments of patients with suspected cardiac sarcoid. *J Am Coll Cardiol* 2014;**63**:329–36
119. Yokoyama R, Miyagawa M, Okayama H, Inoue T, Miki H, Ogimoto A *et al*. Quantitative analysis of myocardial 18F-fluorodeoxyglucose uptake by PET/CT for detection of cardiac sarcoidosis. *Int J Cardiol* 2015;**195**:180–7
120. Yamagishi H, Shirai N, Takagi M, Yoshiyama M, Akioka K, Takeuchi K *et al*. Identification of cardiac sarcoidosis with (13) N-NH(3)/[18F]FDG PET. *J Nucl Med* 2003;**44**:1030–6.
121. Osborne MT1, Hulten EA, Singh A, Waller AH, Bittencourt MS, Stewart GC *et al*. Reduction in ^{18}F-fluorodeoxyglucose uptake on serial cardiac positron emission tomography is associated with improved left ventricular ejection fraction in patients with cardiac sarcoidosis. *J Nucl Cardiol* 2014;**21**:166–74.
122. Ohira H, Birnie DH, Pena E, Bernick J, Mc Ardle B, Leung E *et al*. Comparison of (18)F-fluorodeoxyglucose positron emission tomography (FDG PET) and cardiac magnetic resonance (CMR) in corticosteroid-naive patients with conduction system disease due to cardiac sarcoidosis. *Eur J Nucl Med Mol Imaging* 2016;**43**:259–69.
123. Leask A. The role of endothelin-1 signaling in the fibrosis observed in systemic sclerosis. *Pharmacol Res* 2011;**63**:502–3.
124. Tyndall AJ, Bannert B, Vonk M, Airo P, Cozzi F, Carreira PE *et al*. Causes and risk factors for death in systemic sclerosis: a study from the EULAR Scleroderma Trials and Research (EUSTAR) database. *Ann Rheum Dis* 2010;**69**:1809–15.
125. Follansbee WP, Miller TR, Cirtoss EI, Orie JE, Bernstein RL, Kiernan JM *et al*. A controlled clinicopathologic study of myocardial fibrosis in systemic sclerosis (scleroderma). *J Rheumatol* 1990;**17**:656–62.
126. Meune C, Avouac J, Wahbi K, Cabanes L, Wipff J, Mouthon L *et al*. Cardiac involvement in systemic sclerosis assessed by tissue-doppler echocardiography during routine care: a controlled study of 100 consecutive patients. *Arthritis Rheum* 2008;**58**:1803–9.
127. Allanore Y, Meune C, Vonk MC, Airo P, Hachulla E, Caramaschi P *et al*. Prevalence and factors associated with left ventricular dysfunction in the EULAR Scleroderma Trial and Research group (EUSTAR) database of patients with systemic sclerosis. *Ann Rheum Dis* 2010;**69**:218–21.
128. D'Andrea A, Stisi S, Bellissimo S, Vigorito F, Scotto di Uccio F, Tozzi N *et al*. Early impairment of myocardial function in systemic sclerosis: non-invasive assessment by Doppler myocardial and strain rate imaging. *Eur J Echocardiogr* 2005;**6**:407–18.
129. Yiu KH, Schouffoer AA, Marsan NA, Ninaber MK, Stolk J, Vlieland TV *et al*. Left ventricular dysfunction assessed by speckle-tracking strain analysis in patients with systemic sclerosis. *Arthritis Rheum* 2011;**63**:3969–78.
130. Mueller KA, Mueller II, Eppler D, Zuern CS, Seizer P, Kramer U *et al*. Clinical and histopathological features of patients with systemic sclerosis undergoing endomyocardial biopsy. *PLoS One* 2015;**10**:e0126707.
131. Hachulla AL, Launay D, Gaxotte V, deGroote P, Lamblin N, Devos P *et al*. Cardiac magnetic resonance imaging in systemic sclerosis: a cross-sectional observational study of 52 patients. *Ann Rheum Dis* 2009;**68**:1878–84.
132. Ugander M, Oki AJ, Hsu LY, Kellman P, Greiser A, Aletras AH *et al*. Extracellular volume imaging by magnetic resonance imaging provides insights into overt and sub-clinical myocardial pathology. *Eur Heart J* 2012;**33**:1268–78.
133. Barison A, Gargani L, De Marchi D, Aquaro GD, Guiducci S, Picano E *et al*. Early myocardial and skeletal muscle interstitial remodelling in systemic sclerosis: insights from extracellular volume quantification using cardiovascular magnetic resonance. *Eur Heart J Cardiovasc Imaging* 2015;**16**:74–80.
134. Thuny F, Lovric D, Schnell F, Bergerot C, Ernande L, Cottin V *et al*. Quantification of myocardial extracellular volume fraction with cardiac MR imaging for early detection of left ventricle involvement in systemic sclerosis. *Radiology* 2014;**271**:373–80.
135. Follansbee WP, Curtiss EI, Medsger TA Jr, Steen VD, Uretsky BF, Owens GR *et al*. Physiologic abnormalities of cardiac function in progressive systemic sclerosis with diffuse scleroderma. *N Engl J Med* 1984;**310**:142–8.
136. Lancellotti P, Nkomo VT, Badano LP, Bergler-Klein J, Bogaert J, Davin L *et al*. Expert consensus for multi-modality imaging evaluation of cardiovascular complications of radiotherapy in adults: a report from the European Association of Cardiovascular Imaging and the American Society of Echocardiography. *Eur Heart J Cardiovasc Imaging* 2013;**14**:721–40.
137. Messroghli D, Nordmeyer S, Dietrich T, Dirsch O, Kaschina E, Savvatis K *et al*. Assessment of diffuse myocardial fibrosis in rats using small-animal Look-Locker inversion recovery T1 mapping. *Circ Cardiovasc Imaging* 2011;**4**:636–40.
138. Constine L, Schwartz R, Savage D, King V, Muhs A. Cardiac function, perfusion, and morbidity in irradiated long-term survivors of Hodgkin's disease. *Int J Radiat Oncol Biol Phys* 1997;**39**:897–906.
139. Marks L, Yu X, Prosnitz R, Zhou SM, Hardenbergh P, Blazing M *et al*. The incidence and functional consequences of RT-associated cardiac perfusion defects. *Int J Radiat Oncol Biol Phys* 2005;**63**:214–23.
140. Plana JC, Galderisi M, Barac A, Ewer MS, Ky B, Scherrer-Crosbie M *et al*. Expert consensus for multimodality imaging evaluation of adult patients during and after cancer therapy: a report from the American Society of Echocardiography and the European Association of Cardiovascular Imaging. *Eur Heart J Cardiovasc Imaging* 2014;**15**:1063–93.
141. Dato I. How to recognize endomyocardial fibrosis? *J Cardiovasc Med* 2015;**16**:547–51.
142. Mocumbi AO. Endomyocardial fibrosis: A form of endemic restrictive cardiomyopathy. *Glob Cardiol Sci Pract* 2012;**2012**:11.

143. Bukhman G, Ziegler J, Parry E. Endomyocardial fibrosis: still a mystery after 60 years. *PLoS Negl Trop Dis* 2008;**2**:e97.
144. Mocumbi AO, Carrilho C, Sarathchandra P, Ferreira MB, Yacoub M, Burke M. Echocardiography accurately assesses the pathological abnormalities of chronic endomyocardial fibrosis. *Int J Cardiovasc Imaging* 2011;**27**:955–64.
145. Mocumbi AO, Ferreira MB, Sidi D, Yacoub MH. A population study of endomyocardial fibrosis in a rural area of Mozambique. *N Engl J Med* 2008;**359**:43–9.
146. Kharabish A, Haroun D. Cardiac MRI findings of endomyocardial fibrosis (Loeffler's endocarditis) in a patient with rheumatoid arthritis. *J Saudi Heart Assoc* 2015;**27**:127–31.
147. Schneeweis C, Berger A, Kelle S, Fleck E, Gebker R. Endomyocardial fibrosis in patients with confirmed Churg_Strauss syndrome. *Rheumatology* 2014;**53**: 84.
148. Maia CP, Gali LG, Schmidt A, de Almeida Filho OC, Santos MK *et al*. A challenging differential diagnosis: distinguishing between endomyocardial fibrosis and apical hypertrophic cardiomyopathy. *Echocardiography* 2016;**33**:1080–4.
149. Cury R, Abbara S, Sandoval LJ, Houser S, Brady T and Palacios IF. Visualization of endomyocardial fibrosis by delayed-enhancement magnetic resonance. *Imaging Circulation* 2005;**111**:e115–7.
150. Salemi VMC, Rochitte CE, Shiozaki AA, Andrade JM, Parga JR, de Ávila LF *et al*. Late gadolinium enhancement magnetic resonance imaging in the diagnosis and prognosis of endomyocardial fibrosis patients. *Circ Cardiovasc Imaging* 2011;**4**:304–11.
151. Roper D, Hillier SD, Burstow DJ, Platts D. Non-tropical endomyocardial fibrosis associated with sarcoidosis. *Eur Heart J Cardiovasc Imaging* 2014;**15**: 472.
152. Seguela PE, Iriart X, Acar P, Montaudon M, Roudaut R, Thambo JB. Eosinophilic cardiac disease: molecular, clinical and imaging aspects. *Arch Cardiovass Dis* 2015;**108**:258–68.
153. Al Ali AM, Straatman LP, Allard MF, Ignaszewski AP. Eosinophilic myocarditis: case series and review of literature. *Can J Cardiol* 2006;**22**:1233–7.
154. Ommen SR, Seward JB, Tajik AJ. Clinical and echocardiographic features of hypereosinophilic syndromes. *Am J Cardiol* 2000;**1**:110–3.
155. Simonnet B, Jacquier A, Salaun E, Hubert S, Habib G. Cardiac involvement in hypereosinophilic syndrome: role of multimodality imaging. *Eur Heart J Cardiovasc Imaging* 2015;**16**:228.
156. Acquatella H, Schiller NB, Puigbó JJ, Gómez-Mancebo JR, Suarez C, Acquatella G. Value of two-dimensional echocardiography in endomyocardial disease with and without eosinophilia. A clinical and pathologic study. *Circulation* 1983;**67**:1219–26.
157. Rotoli B, Catalano L, Galderisi M, Luciano L, Pollio G, Guerriero A *et al*. Rapid reversion of Loeffler's endocarditis by imatinib in early stage clonal hypereosinophilic syndrome. *Leuk Lymphoma* 2004;**45**:2503–7.
158. Puvaneswary M, Joshua F, Ratnarajah S. Idiopathic hypereosinophilic syndrome: magnetic resonance imaging findings in endomyocardial fibrosis. *Australas Radiol* 2001;**45**:524–7.
159. Porto AG, McAlindon E, Hamilton M, Manghat N, Bucciarelli-Ducci C. Diagnosing cardiac involvement in the hypereosinophilic syndrome by cardiac magnetic resonance. *Am J Cardiol* 2013;**112**:135–6.
160. Pillar N, Halkin A, Aviram G. Hypereosinophilic syndrome with cardiac involvement: early diagnosis by cardiac magnetic resonance imaging. *Can J Cardiol* 2012;**515**:e11–3.
161. ten Oever J, Theunissen LJ, Tick LW, Verbunt RJ.Cardiac involvement in hypereosinophilic syndrome. *Neth J Med* 2011;**69**:240.
162. Haugaa KH, Bergestuen DS, Sahakyan LG, Skulstad H, Aakhus S, Thiis-Evensen E *et al*. Evaluation of right ventricular dysfunction by myocardial strain echocardiography in patients with intestinal carcinoid disease. *J Am Soc Echocardiogr* 2011;**24**:644–50.
163. Modlin IM, Shapiro MD, Kidd M. Carcinoid tumors and fibrosis: an association with no explanation. *Am J Gastroenterol* 2004;**99**:2466–78.
164. Connolly HM, Pellikka PA. Carcinoid heart disease. *Curr Cardiol Rep* 2006;**8**:96–101.
165. Pellikka PA, Tajik AJ, Khandheria BK, Seward JB, Callahan JA, Pitot HC *et al*. Carcinoid heart disease. Clinical and echocardiographic spectrum in 74 patients. *Circulation* 1993;**87**:1188–96.
166. Urheim S, Edvardsen T, Torp H, Angelsen B, Smiseth OA. Myocardial strain by Doppler echocardiography. Validation of a new method to quantify regional myocardial function. *Circulation* 2000;**102**:1158–64.
167. Zahid W, Bergestuen D, Haugaa KH, Ueland T, Thiis-Evensen E, Aukrust P *et al*. Myocardial function by two-dimensional speckle tracking echocardiography and activin A may predict mortality in patients with carcinoid intestinal disease. *Cardiology* 2015;**132**:81–90.
168. Moerman VM, Dewilde D, Hermans K. Carcinoid heart disease: typical findings on echocardiography and cardiac magnetic resonance. *Acta Cardiol* 2012;**67**:245–8.
169. Nebigil CG, Etienne N, Messaddeq N, Maroteaux L. Serotonin is a novel survival factor of cardiomyocytes: mitochondria as a target of 5-ht2b receptor signaling. *FASEB J* 2003;**17**:1373–5.
170. Hutcheson JD, Setola V, Roth BL, Merryman WD. Serotonin receptors and heart valve disease–it was meant 2b. *Pharmacol Ther* 2011;**132**:146–57.
171. Fielden MR, Hassani M, Uppal H, Day-Lollini P, Button D, Martin RS *et al*. Mechanism of subendocardial cell proliferation in the rat and relevance for understanding drug-induced valvular heart disease in humans. *Exp Toxicol Pathol* 2010;**62**:607–13.
172. Fowles RE, Cloward TV, Yowell RL. Endocardial fibrosis associated with fenfluramine-phentermine. *N Engl J Med* 1998;**338**:1316.
173. Szymanski C, Marechaux S, Bruneval P, Andrejak M, de Montpréville VT, Belli E *et al*. Sub obstruction of left outflow tract secondary to benfluorex-induced endocardial fibrosis. *IJC Heart Vasculature* 2015;**9**:67–9
174. Vaitkus PT, Kussmaul WG. Constrictive pericarditis versus restrictive cardiomyopathy: a reappraisal and update of diagnostic criteria. *Am Heart J* 1991;**122**:1431–41.
175. Shabetai R. Pathophysiology and differential diagnosis of restrictive cardiomyopathy. *Cardiovasc Clin* 1988;**19**:123–32.
176. Kusunose K, Dahiya A, Popović ZB, Motoki H, Alraies MC, Zurick AO *et al*. Biventricular mechanics in constrictive pericarditis comparison with restrictive cardiomyopathy and impact of pericardiectomy. *Circ Cardiovasc Imaging* 2013;**6**:399–406.
177. Welch TD, Ling LH, Espinosa RE, Anavekar NS, Wiste HJ, Lahr BD *et al*. Echocardiographic diagnosis of constrictive pericarditis. Mayo clinic criteria. *Circ Cardiovasc Imaging* 2014;**7**:526–34.
178. Ha JW, Ommen SR, Tajik AJ, Barnes ME, Ammash NM, Gertz MA *et al*. Differentiation of constrictive pericarditis from restrictive cardiomyopathy using mitral annular velocity by tissue Doppler echocardiography. *Am J Cardiol* 2004;**94**:316–9.
179. Ha JW, Oh JK, Ommen SR, Ling LH, Tajik AJ. Diagnostic value of mitral annular velocity for constrictive pericarditis in the absence of respiratory variation in mitral inflow velocity. *J Am Soc Echocardiogr* 2002;**15**:1468–71.
180. Sengupta PP, Mohan JC, Mehta V, Arora R, Pandian NG, Khandheria BK. Accuracy and pitfalls of early diastolic motion of the mitral annulus for diagnosing constrictive pericarditis by tissue Doppler imaging. *Am J Cardiol* 2004;**93**:886–90.
181. Rajagopalan N, Garcia MJ, Rodriguez L, Murray RD, Apperson-Hansen C, Stugaard M *et al*. Comparison of new Doppler echocardiographic methods to differentiate constrictive pericardial heart disease and restrictive cardiomyopathy. *Am J Cardiol* 2001;**87**:86–94.
182. Amaki M, Savino J, Ain DL, Sanz J, Pedrizzetti G, Kulkarni H *et al*. Diagnostic concordance of echocardiography and cardiac magnetic resonance-based tissue tracking for differentiating constrictive pericarditis from restrictive cardiomyopathy. *Circ Cardiovasc Imaging* 2014;**7**:819–27.
183. Adler Y, Charron P, Imazio M, Badano L, Baron-Esquivias G, Bogaert J *et al*. 2015 ESC Guidelines for the diagnosis and management of pericardial diseases: The Task Force for the Diagnosis and Management of Pericardial Diseases of the European Society of Cardiology (ESC)Endorsed by: The European Association for Cardio-Thoracic Surgery (EACTS). *Eur Heart J* 2015;**36**:2921–64.
184. Talreja DR, Edwards WD, Danielson GK, Schaff HV, Tajik AJ, Tazelaar HD *et al*. Constrictive pericarditis in 26 patients with histologically normal pericardial thickness. *Circulation* 2003;**108**:1852–7.
185. Yared K, Baggish AL, Picard MH, Hoffmann U, Hung J. Multimodality imaging of pericardial diseases. *JACC Cardiovasc Imaging* 2010;**3**:650–60.
186. Elliott PM, Anastasakis A, Borger MA, Borggrefe M, Cecchi F, Charron P *et al*. 2014 ESC Guidelines on diagnosis and management of hypertrophic cardiomyopathy: the Task Force for the Diagnosis and Management of Hypertrophic Cardiomyopathy of the European Society of Cardiology. *Eur Heart J* 2014;**35**:2733–92.
187. Olivotto I, Maron BJ, Appelbaum E, Harrigan CJ, Salton C, Gibson CM *et al*. Spectrum and clinical significance of systolic function and myocardial fibrosis assessed by cardiovascular magnetic resonance in hypertrophic cardiomyopathy. *Am J Cardiol* 2010;**106**:261–7.
188. Biagini E, Spirito P, Rocchi G, Ferlito M, Rosmini S, Lai F *et al*. Prognostic implications of the Doppler restrictive filling pattern in hypertrophic cardiomyopathy. *Am J Cardiol*;**104**:1727–31.
189. Melacini P, Basso C, Angelini A, Calore C, Bobbo F, Tokajuk B *et al*. Clinicopathological profiles of progressive heart failure in hypertrophic cardiomyopathy. *Eur Heart J* 2010;**31**:2111–23.
190. Nistri S, Olivotto I, Betocchi S, Losi MA, Valsecchi G, Pinamonti B *et al*. Prognostic significance of left atrial size in patients with hypertrophic cardiomyopathy (from the Italian Registry for Hypertrophic Cardiomyopathy). *Am J Cardiol* 2006;**98**:960–5.

191. Maron BJ, Spirito P. Implications of left ventricular remodeling in hypertrophic cardiomyopathy.*Am J Cardiol* 1998;**81**:1339–448.
192. Olivotto I, Cecchi F, Poggesi C, Yacoub MH. Patterns of disease progression in hypertrophic cardiomyopathy: an individualized approach to clinical staging. *Circ Heart Fail* 2012;**5**:535–46.
193. Habib G, Charron P, Eicher JC, Giorgi R, Donal E, Laperche T *et al*. Working Groups 'Heart Failure and Cardiomyopathies' and 'Echocardiography' of the French Society of Cardiology. Isolated left ventricular non-compaction in adults: clinical and echocardiographic features in 105 patients. Results from a French registry. *Eur J Heart Fail* 2011;**13**:177–85.
194. Rapezzi C, Leone O, Ferlito M, Biagini E, Coccolo F, Arpesella G. Isolated ventricular non-compaction with restrictive cardiomyopathy. *Eur Heart J* 2006;**27**:1927.